Cross-hierarchical Corticothalamic Plasticity in the Mouse Visual System

Chrysoula Giasafaki
St Cross College

A thesis submitted for the degree of
Master of Science by Research

Word count: 16453

Trinity Term 2019

Table of Contents

Abstract

Almost all sensory information reached our brain via the thalamus. The thalamus is considered the relay center for sensory information to the cortex and has an essential role in the regulation of fundamental brain processes, including sleep, alertness, consciousness and cognition, via various distinct nuclei. Specifically in the visual system, inputs from the retina project to the “first-order” dorsal lateral geniculate nucleus (dLGN) of the thalamus, which projects to the primary visual cortex (V1). Layer V neurons selectively project to the “higher-order” lateral posterior nucleus (LP) and do not normally innervate dLGN. It has been recently proposed by Grant et al., (2016), that layer V projections rewire to innervate dLGN fter monocular enucleation (MoE); however, the cortical origin of these projections has not been determined. In my study, I examined neuronal rewiring of cortical layer V projections and their plasticity to structurally rearrange following neonatal MoE. After performing MoE in layer V-labelled transgenic mice (Rbp4-Cre::tdTomato) at birth, I studied the effects on the ingrowth of tdTomato-labelled corticofugal projections into visual thalamic nuclei, the dLGN and the LP. In order to investigate the corical origin of aberrant layer V projections in the sensory deprived dLGN, I performed AAV viral injections in the primary visual (V1) and somatosensory (S1) cortices of adult Rbp4-Cre::tdTomato mice (n=3 for V1, n=3 for S1) that had been monocularly enucleated at birth. My findings indicate innervation of layer V corticothalamic (GFP+) axons in the lower part of dLGN and LP only from V1 with formation of aberrant side branches and VGluT1+ boutons in the deprived dLGN. No alterations in the S1 projections to thalamus were observed following MoE with S1 axons completely bypassing dLGN. However, projections from A1 or other sources, such as secondary cortical areas, should also be further investigated. What is more, an increase in the bouton density was identified in the dLGN after input deprivation. Additionally, I examined the molecular changes induced by MoE in the thalamus at P8 by *in situ* hybridization and confirmed differential pattern of expression in control and deprived dLGN (n=3). Otx2 and Cbln2 showed increased expression in deprived dLGN accompanied by upregulation of gene expression in vLGN. Kcnk9 and Calb2 were downregulated in dLGN upon enucleation, also showing increased expression in vLGN. EphA5 was differentially expressed in dLGN and LP in control hemisphere with dLGN showing stronger labelling, whereas this difference was no longer evident after enucleation in dLGN of reduced volume. All the aforementioned results demonstrate the necessity of peripheral input for proper layer V axonal ingrowth, synaptic formation and transcriptional profile of the dlGN and might indicate its importance in the establishment of the specific characteristics of each order of thalamic nuclei.

Statement of Authorship

The work presented in this thesis is my own with the following exceptions:

1. Section 3.2.: The intracerebral viral injections in V1 and S1 were performed by Dr Anna Hoerder-Suabedissen from the Molnár laboratory. Tissue processing, immunohistochemistry, imaging and statistical analysis were all my own work.

2. Section 3.3.: The microarray data analysis of control and enucleated dLGN at P6 is the work of Dr Eleanor Grant, former member of the Molnár laboratory, and was previously presented in her DPhil thesis in 2014.

3. Section 3.3.: The probes Otx2, Kcnk9 and EphrinA5 used for the *in situ* hybridization experiments were provided by Dr Shuichi Hayashi from the Molnár laboratory. The *in situ* hybridization experiments, imaging and statistical analysis were my own work.

Acknowledgements

I would like to express my gratitude to my supervisor, Professor Zoltán Molnár, for giving me the opportunity to join his laboratory to pursue my research. I really enjoyed his enthusiastic mentorship, our inspiring meetings for scientific brainstorming, and most of all his support, patience and advices in a professional and personal level. Zoltán is a great supervisor with an amazing personality, always advising me for my best interest and offering me countless opportunities.

I would also like to thank my secondary supervisor, Dr Anna Hoerder-Suabedissen, for all the time she invested on teaching me many laboratory techniques, having long discussions with me that helped me progress with my project, and for always being very considerate and supportive on difficult situations.

Throughout the year, the members of the Molnár laboratory have been next to me supporting me in my research and on a personal level. To Dr Shuichi Hayashi, for his essential help with all the *in situ* experiments and his day-to-day supervision. I particularly enjoyed working with him as well as our many discussions about our research, which have helped me advance my critical thinking as a scientist. To Kris, for answering all my questions for the everyday work in the laboratory and her thoughtfulness and willingness to always help us. Also, to Jan and Jolande, my perfect labmates that were always there for me, for the long nights and weekends in the lab, the endless chats in the office, the beers and our fun activities around Oxford.

Finally, I wouldn’t have made it without the support from my friends Laura and Katerina, my DPAG partners in crime, my dear friend Kika, whom I met in the Molnár laboratory and has been like family to me ever since, my new labmates in the Lopez-Bendito lab, who encouraged me while I was writing my thesis, and of course my family and friends back in Greece, who are always very proud of me, put up with me and support me every step on the way.

List of abbreviations

AAV	adeno-associated virus
BDNF	brain derived neurotrophic factor
Calb2	calbindin 2
Cbln2	cerebellin 2 precursor protein
CTAs	corticothalamic axons
dLGN	dorsal Lateral Geniculate Nucleus
EphA5	ephrinA5
Egr1	early growth response 1
Egr2	early growth response 2
EPSC	excitatory post-synaptic current
EPSP	excitatory post-synaptic potential
Fam19a4	family with sequence similarity 19, member A4
FO	first-order
HO	higher-order
Igf1	insulin-like growth factor 1
Igf2	insulin-like growth factor 2
IN	interneuron
IPSC	inhibitory post-synaptic current
IPSP	inhibitory post-synaptic potential
Kcnk9	potassium channel, subfamily K, member 9
Kcnn3	potassium intermediate/small conductance calcium-activated channel, subfamily N, member 3
LP	Lateral posterior thalamic nucleus
MGN	medial geniculate nucleus
MoE	monocular enucleation
Moxd1	monooxygenase, DBH-like 1

Myot	Myotilin
ON	Optic Nerve layer of superior colliculus
Osbpl3	oxysterol binding protein-like 3
Otx2	orthodenticle homologue 2 (Drosophila)
Po	posterior thalamic nucleus
pTh-C	caudal prethalamic domain
pTh-R	rostral prethalamic domain
SC	superior colliculus
TCAs	thalamocortical axons
TRN	thalamic reticular nucleus
VGluT1	vesicular glutamate transporter 1
vLGN	ventral Lateral Geniculate Nucleus
VPM	ventral posteromedial nucleus

1. Introduction

The thalamus is an evolutionarily conserved structure situated centrally in the brain above the brain stem and surrounded by the cerebral cortex. It is widely implicated in the regulation of fundamental brain processes including sleep, alertness, consciousness and cognition via various distinct nuclei (Sherman and Guillery, 2002; Jones 2007).

The thalamus is considered the relay center for sensory information to the cortex. However, it is not just a simple and passive relay station, but instead is implicated in various dynamic processes that determine the nature of most afferent information conveyed to the cortex, thus affecting behaviour (Sherman and Guillery, 1996). It is subdivided into more than 40 nuclei, which are distinguished according to their distinct function, cytoarchitecture, anatomical connectivity and gene expression patterns (Jones, 2007). Extensive reciprocal connections between the thalamus and the cortex are established through the formation of thalamocortical and corticothalamic projections that convey sensory and motor information necessary for cortical activity from the periphery in sensory areas and associative brain regions (Deck et al, 2013; Hunnicutt et al, 2014). Additionally, the thalamus is involved in the regulation of cortico-cortical communication and synchrony (Sherman and Guillery, 2005; Theyel et al, 2010; Saalman et al, 2012), motor control and establishment of cortical states. The area-specific thalamocortical projections also participate in the establishment of cortical patterning and cytoarchitectonic differentiation during development (O-leary, 1989; Chou et al, 2013), all of which indicate its importance in further understanding perception and cognition. The sensory input to the thalamus is outnumbered by the corticothalamic projections by 1 to 10 (Sherman and

Guillery, 2005). The formation of the reciprocal connectivity between the thalamus and the cortex and its subsequent experience-dependent refinement results to the orchestrated development of sensory circuits (Katz and Shatz, 1996; Sur and Rubenstein, 2005).

Although the anatomical organization of multiple thalamic nuclei has been extensively studied, the mechanisms underlying their development and establishment are still largely unknown. Properties of thalamic nuclei are not determined by the connections they receive and the activity patterns they produce. The early specification of thalamic relay cells precedes the establishment of connections, raising questions regarding the degree to which developing thalamic nuclei are committed to their molecular fates, connections and functions, as well as their plasticity when confronted with genetic, connectional or other perturbations during development and in adult (Jager et al, 2016).

1.1. Early development of the thalamus

Early in embryonic development, the actions of diffusible signalling molecules, known as morphogens [Bone morphogenetic proteins (BMPs), Wingless-Int proteins (Wnts) and Fibroblast growth factor proteins (Fgfs)],released from local signaling centres lead to the establishment of positional information and the subdivision of the anterior neural plate and neural tube into regions that express different combinations of high-level transcription factors, often referred to as master regulators (Lim and Golden, 2007; Scholpp and Lumsden, 2010; Martinez-Ferre and Martinez, 2012; Chatterjee and Li, 2012; Puelles et al., 2013). These transcription factors specify the spatiotemporal patterning of different brain regions and the identities of the cells that express them, although specification does not mean they are irrevocably committed and subsequent intercellular interactions will be critical determinants (Vue et al, 2013).

Following neural tube closure, along the longitudinal axis of the neuroepithelium, the neural tube's anterior end is subdivided giving rise to the prosencephalon (forebrain) among other brain vesicles, which will further subdivide into the secondary prosencephalon and the diencephalon. According to the "prosomeric model" proposed by Puelles and Rubenstein (2003), along the anteroposterior axis, the diencephalon will then develop into three transverse segments; the pretectum (p1), thalamus (p2) and prethalamus (p3), with distinct morphological boundaries and regulatory genes, such as *Pax6*, *Dlx2* and *Wnt3* (Figure 1A). By embryonic day (E)12.5, in mouse brain development, the thalamic formation is completed with thalamic nuclei arising from the alar plate of the thalamic anlage (Puelles and Rubenstein, 2003). The thalamus is topographically determined by specific transcription factors, including *Otx2*, *Irx1*, *Gbx2* and *Pax6*, as well as by the *zona limitans intrathalamica* (ZLI), a forebrain organizing centre that acts as a boundary between thalamic and prethalamic anlagen by promoting Sonic hedgehog *Shh* expression (Nakagawa and O'Leary, 2001; Price et al, 2002).

In rodents, thalamic neurogenesis takes place in the ventricular zone through a specific, narrow timeframe throughout embryonic development (E10.5 to E16.5) (Argevine, 1970). The thalamus develops from two diencephalic progenitor domains distinguished by their expression of different combinations of transcription factors: the caudal prethalamic domain (pTh-C), which is a relatively small region that lies caudal to the ZLI and expresses *Neurogenin 1* and *2*, *Gbx2*, *Olig3* and *Sox2* amongst others; and the rostral prethalamic domain (pTh-R), which is smaller, lies rostral to pTh-C and expresses *Ascl1, Mash1* and *Nkx2.2* (Figure 1B) (Vue et al, 2007). Previous studies used genetic fate mapping of the mouse brain to demonstrate that all thalamic glutamatergic excitatory neurons are generated from the pTh-C, whereas GABAergic inhibitory interneurons, including Otx2-positive and Sox14-negative, that populate the intergeniculate leaflet (IGL), ventral LGN and thalamic reticular nucleus (TRN) arise from pTh-R and the prethalamus (Vue et al, 2007; Jeong et al, 2011; Inamura et al, 2011; Golding et al, 2014). It has also recently been demonstrated that GABAergic interneurons might originate from the tectum, where Sox14 and Gata2 positive interneurons were identified (Jager et al, 2016).

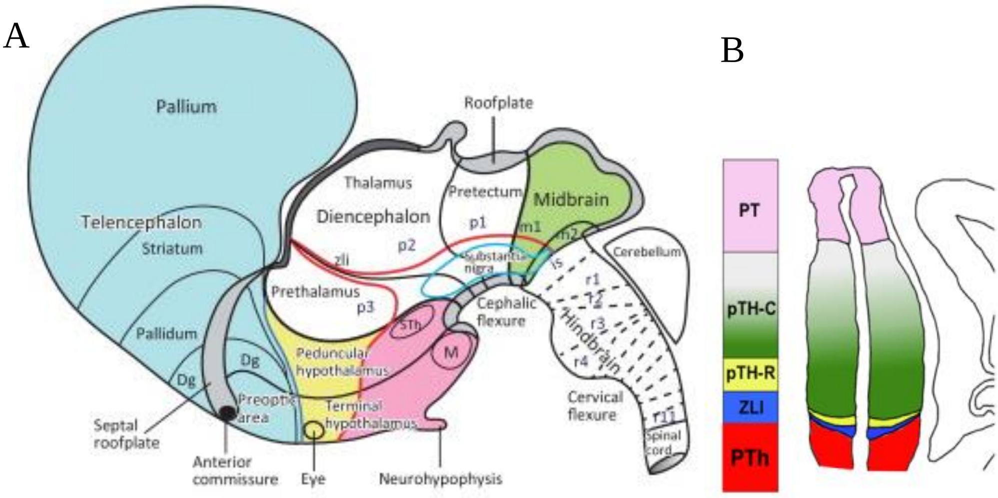

Figure 1.1: **(A)** Schematic representation of the organization of the developing mouse neural tube along the longitudinal axis, following the prosomeric model. Adapted from Puelles et al., 2013. **(B)** Schematic representation of a frontal section of the several diencephalic regions; moving from caudodorsal (top of section) to rostroventral (bottom of section). Abbreviations: PT, Pretectum; ZLI, zona limitans intrathalamica; PTh, Prethalamus. Adapted from Bluske et al, 2012.

1.2. Thalamic nuclei classification

All peripheral sensory information is represented in the thalamus before being transmitted to the cortex, with the exception of olfaction. Sensation begins when peripheral receptors, such as retinal photoreceptors and skin mechanoreceptors, are activated in order to detect external stimuli. Based on the origin of the input they receive, either subcortical (cerebellum, mamillary bodies, basal ganglia) or cortical, thalamic nuclei are classified into “first-order” (FO) and “higher-order” (HO) respectively, a classification conserved across all mammalian species including humans (Sherman and Guillery, 1998; Bickford, 2015). FO (or relay) thalamic nuclei contain core[1] thalamic relay cells that process peripheral information and convey it to the cortex.

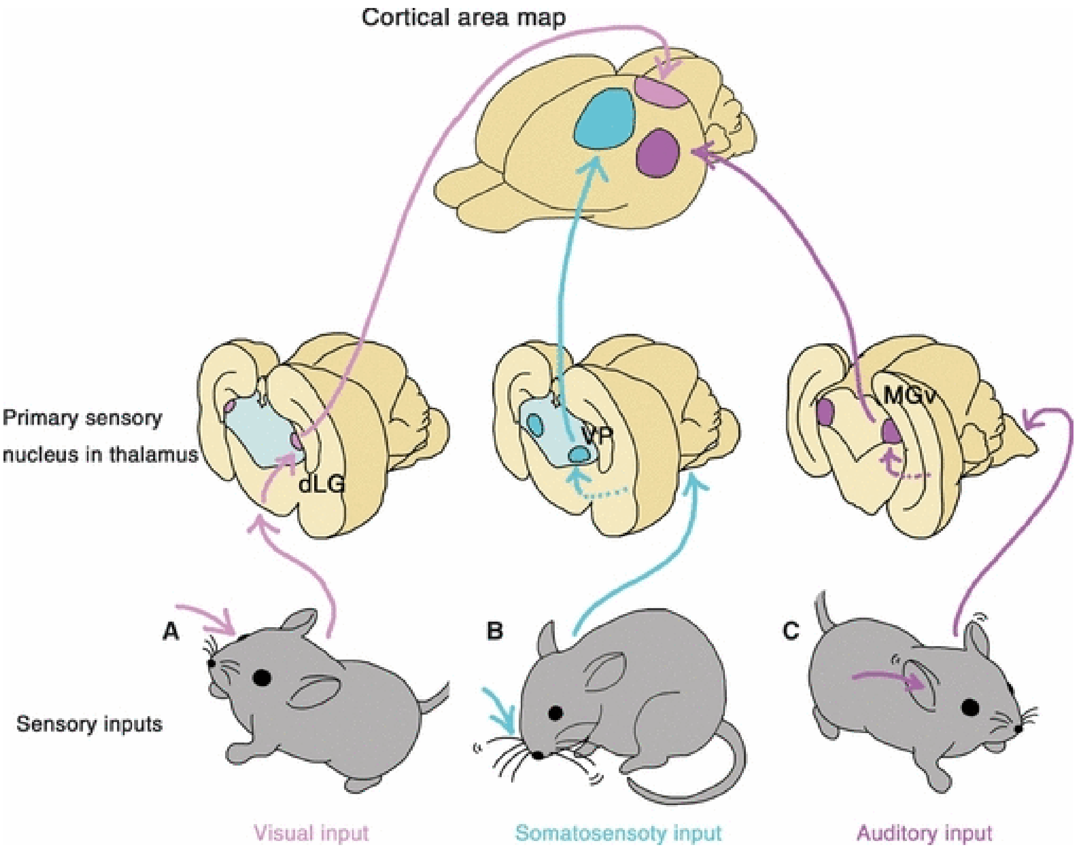

Figure 1.2: **Schema of sensory input pathway in CNS**. (A) Visual information is conveyed to the dLGN in the thalamus and is then relayed to the primary visual cortex. (B) Somatosensory information from rodent whiskers and the skin is sent to the VP nuclear complex via the brainstem and the spinal cord, and reaches the primary somatosensory cortex. (C) Auditory information reaches the inferior colliculus of the midbrain via the cochlear nuclei and superior olivary complex of the brainstem. This information then reaches the MGv in the thalamus and is relayed to the primary auditory cortex. Adapted from Nakawaga and Shimogori (2012).

---

[1] Core thalamocortical cells: Parvalbumin-positive neurons occupying sensory and motor thalamic nuclei and projecting mostly to layer 4 of particular cortical areas.

Retinal input is relayed to the dorsal lateral geniculate nucleus (dLGN), the FO visual nucleus, which then projects to the primary visual cortex (V1) (Le Gros Clark, 1932; Valverde, 1968; Godement et al, 1984). Somatosensory information is conveyed via the trigeminal nucleus to the ventral posterior medial nucleus (VPM), the FO somatosensory nucleus, which then targets the primary somatosensory cortex (S1) (Le Gros Clark, 1932; Reichova and Sherman, 2004). Finally, auditory input is relayed via inferior colliculus (IC) and the cochlear nucleus to the ventral medial geniculate nucleus (MGv), the FO auditory nucleus, which then projects to the primary auditory cortex (A1) (Le Gros Clark, 1932; Sherman and Guillery, 1996; Guillery and Sherman, 2002). From the primary somatosensory cortices, information is projected back to the matrix[2] cells of HO (or association) thalamic nuclei in a modality-specific manner; driver input from V1 is relayed to the visual HO lateral posterior nucleus (LP), from S1 to the somatosensory HO posterior nucleus (Po) and from A1 to the auditory HO dorsal medial geniculate nucleus (MGd), which then project back to their corresponding secondary cortices (Le Gros Clark, 1932; Sherman and Guillery, 1996; Guillery and Sherman, 2002)

1.3. Thalamic neurogenesis and nuclei specification

The mechanisms that generate discrete thalamic nuclei remain poorly understood, mostly due to the complex nuclei arrangement and the short window of neuronal generation in the thalamus. There is evidence that temporal, spatial and lineage-dependent variables are important. Early studies by Altman and Bayer (1988) used [^{3}H]-thymidine birth-dating in rats to show that

---

[2] Matrix thalamocortical cells: Calbindin-positive neurons occupying mainly medial and intralaminar thalamic nuclei and projecting diffusely to superficial cortical layers.

TRN neurons have temporally and spatially diverse origins (Altman and Bayer, 1988a, b, c). Other studies showed that glutamatergic neurons populating FO thalamic nuclei arise from the pTh-C earlier (E10.5-15.5) on average, than those contributing to HO thalamic nuclei (Vue at al, 2007; Nakawaga and Shimogori, 2012; Gezelius et al, 2016), indicating a temporal regulation in the establishment of neuronal diversity in different nuclei.

Interestingly, recent ontogeny studies reported that distinct thalamic nuclei identity and organization is partly dependent on lineage specification (Wong et al, 2018; Shi et al, 2017). Shi et al (2017) suggested that individual progenitors arising from the thalamic VZ produce neurons that are preferentially located in specific sets of thalamic nuclei. These sets of nuclei with distinct ontogeny also exhibit a functional segregation with anterior and medial-dorsal clones occupying sensory-, motor- and cognition-related HO nuclei, whereas the medial-ventral-posterior clone principally clustering to sensory- and motor-related FO nuclei. These results suggested that separation of the sensory- and motor-related nuclei in hierarchy is highly lineage-related (Shi et al, 2017).

Additionally, individual clones occupying either FO or HO thalamic nuclei across modalities frequently clustered together indicating a cross-modal framework of progenitor origin. This is consistent with previous anatomical studies by Clasca et al (2012) demonstrating that FO nuclei are largely occupied by core TC cell type, while HO nuclei by matrix TC cells (Clasca et al, 2012), as well as with genetic studies (Frangeul et al, 2016) showing that FO nuclei are transcriptionally more similar to each other across modalities than they are to HO nuclei of the same modality.

On the other hand, Wong et al (2018) showed a pattern of prolonged specification of nuclear fate by identifying intermediate progenitor cells producing neurons that populate multiple nuclei. What is more, their analysis revealed rostrally-located clones occupying FO sensory nuclei, whereas caudally-located clones contributed to HO caudo-dorsal nuclei, indicating that the location of progenitor cells predicts the set of nuclei they preferentially occupy (Wong et al, 2018). Overall, these distinct progenitor origins of neurons occupying FO and HO thalamic nuclei might indicate their contribution in the development of different morphology, functionality and anatomical connectivity.

1.4. Development of thalamocortical and corticothalamic projections

In rodents, during the second and third weeks of gestation, TC and CT afferents start to develop and grow towards their target areas following specific pathways established by molecular guidance cues. At E13, TCAs initially grow through the prethalamus, and then turn dorso-laterally at the diencephalic-telencephalic boundary (DTB) in order to enter the internal capsule (IC) (Erzurumlu and Jhaveri, 1992 Jacobs et al, 2007). There, they wait for a day before entering at the pallial-subpallial boundary (PSPB) at E15. At the same timepoint, CTAs have already projected from the preplate ventro-laterally to reach the PSPB at E14, where they pause for a day (Noctor et al, 2004; Molyneaux et al, 2007). During this waiting period in the PSPB, TC and CT axons intermingle and continue growing in close vicinity eventually navigating each other to their corresponding target (Molnár et al, 1998a, b; Deck et al, 2013). At E16.5, both TCAs and CTAs have crossed the PSPB with the first reaching the cortex at the level of the subplate and waiting there until P0, when they finally enter Layer IV of the cortex, while the latter project to the TRN, where their second pause occurs before entering the thalamus at E17.5. By P4, TCAs start the refinement of their terminals and CTAs start to invade their target thalamic nuclei (Price et al, 2006; Molnár et al, 2012; Garel and Lopez-Bendito, 2014).

The pathfinding of TC and CT axons to their corresponding targets is highly regulated by interactions of attractant molecules and their receptors, such as Netrin 1 and DCC, members of the Eph family and their ligands, Semaphorin6A, Ebf1, which guide axons to the subpallium, as well as repulsive guidance cues, such as Slits and their receptors Robos, Semaphorins with Plexins, that deviate axons from the hypothalamus in order to enter the DTB (Molnár et al, 2012; Garel and Lopez-Bendito, 2014). Loss of function studies have shown that TCAs fail to form a topographic anatomical or functional map en route to the neocortex, which suggests the necessity of these guidance cues for the proper pathfinding of axons to their targets (Deck et al, 2013; Lokmane et al, 2013).

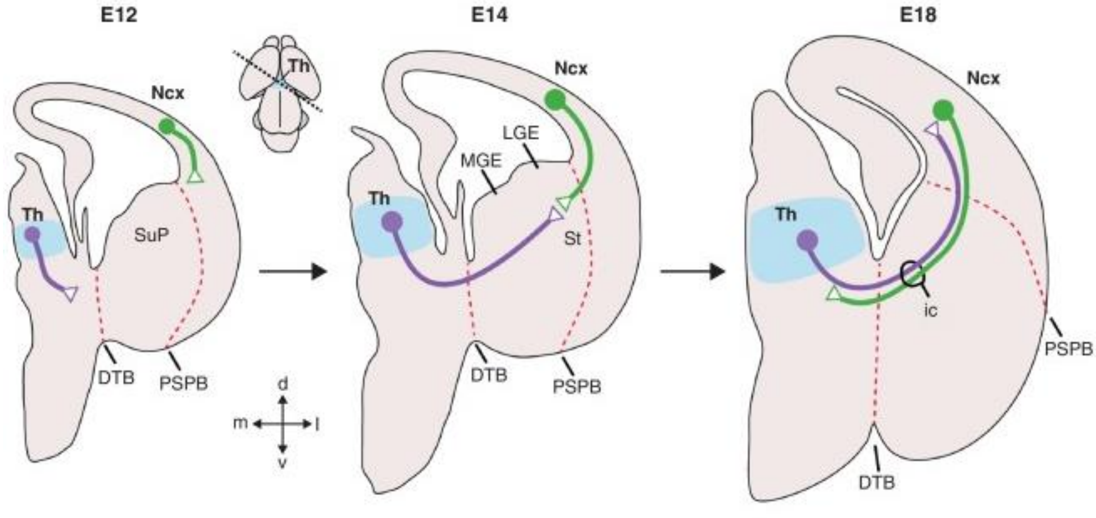

Figure 1.3: **The development of thalamocortical and corticothalamic projections.** Schematic representation showing the time course of development and progression of thalamocortical axons (TCAs, purple) and corticothalamic subplate axons (green) in brain hemisections between E12 and E18 in mice. Axons cross several major boundaries, including the diencephalic/telencephalic (DTB) and pallial/subpallial boundaries (PSPB), and travel internally through the subpallium (SuP) including the medial and lateral ganglionic eminences (MGE and LGE). TCAs and subplate axons

meet in the lateral part of the striatum (St) to form together the internal capsule (ic). Adapted from Garel and Lopez-Bendito, 2014.

1.4.1. Corticothalamic circuit

CT projections outnumber TC projections by 10-fold comprising more than 50% of synaptic input to thalamic relay neurons. They play an essential role in the regulation of the thalamic input required for the processing and integration of complex information to the cortex (Jones, 2002). Although much attention has focused on understanding the mechanisms governing TC circuit formation and axon guidance to their cortical target, little is known about development and regulation of CT projections (Lopez-Bendito and Molnár, 2003).

Input from different sensory modalities follows a highly specific and conserved cortico-thalamo-cortical circuit motif**.** Information originating from the periphery or subcortical areas relays on the core cells of FO thalamic nuclei, which project to Layer IV of their corresponding primary cortices. Following, from Layer Vb pyramidal cells of the primary cortical area, corticofugal projections innervate the matrix cells of their respective HO thalamic nuclei. Layer V corticothalamic projections are collaterals of long-range corticofugal axons reaching the brainstem and spinal cord amongst others, without reaching to the TRN (Deschênes et al. 1994). Layer V cells projecting to LP also showed arborization into the superior colliculus (Rouiller and Welker, 1991; Deschênes et al. 1994). What is more, HO nuclei receive most of their input from layer V corticospinal and corticobulbar projections (Sherman and Guillery, 2002). Axons from HO nuclei then project back to Layer IV of their secondary cortices regulating thalamocortical communication. Additionally, projections from Layer IV reach layer II/III of respective primary and secondary cortices, such as primary motor cortex (M1) and S2 and V2, respectively, thus facilitating cortico-cortical communication (Jones, 2002; Sherman and Guillery, 2002; Grant et al, 2012). Finally, layer VI neurons project subcortically to the spinal cord and all thalamic nuclei, providing modulatory feedback input to thalamic relay cells in both first-order and higher-order thalamic nuclei (Olsen et al, 2012; Lam and Sherman, 2013; Crandall et al, 2015). Layer VI axons also provide modulatory input to TRN via collateral projections, initiating an inhibitory feedforward circuit that regulates thalamic neural activity (Jones, 2002; Sherman and Guillery, 2013).

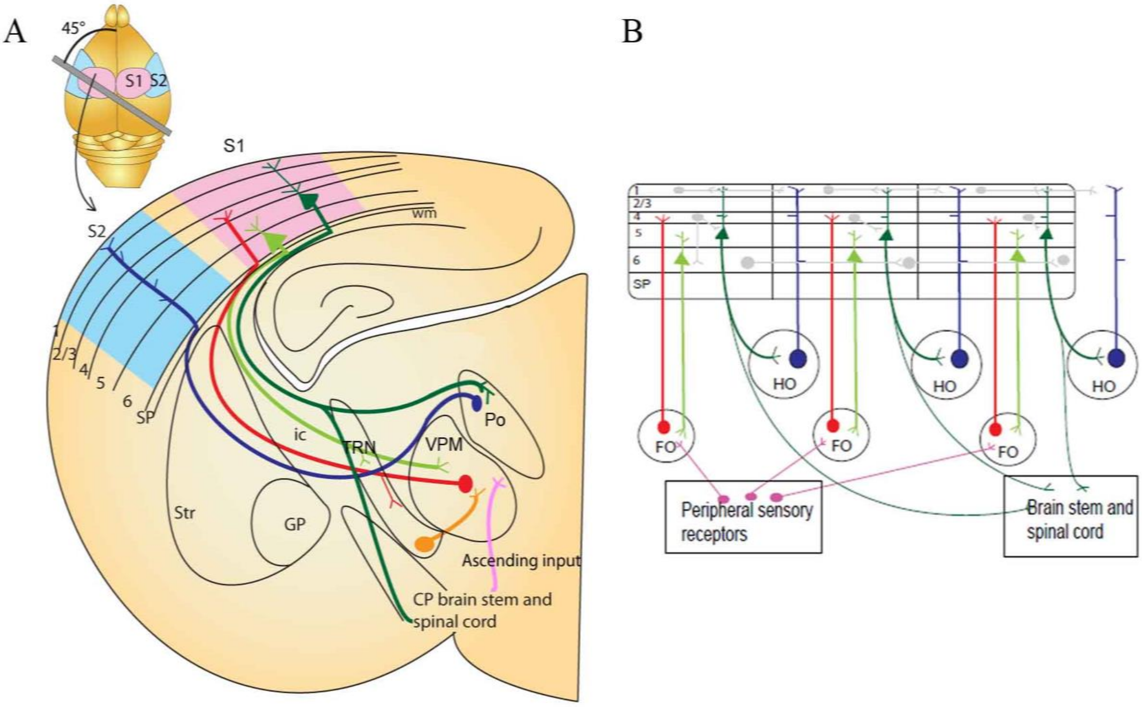

Figure 1.4: The cortico-thalamo-cortical circuit. Coronal schematic representation of the connectivity between the cortex and thalamus using the somatosensory system as an example. The first-order VPM thalamic nucleus receives somatosensory peripheral input (pink). The VPM then projects axons (red) to layer 4 of the primary somatosensory cortex (S1; light blue). Layer 6 "modulator" neurons (light green) in S1 project back to the VPM. Layer 5 neurons (dark green) in S1 project subcortically making collateral branches to the higher-order posterior thalamic nucleus (Po). Po then project (dark blue) to an area of cortex that is different from the one it received input from (for example S2; light pink), generating an open cortico-thalamo-cortical loop. **(B)** Schematic illustration of the possible functional circuits generated by this reoccurring open loop connectivity. Sensory information is relayed through the first order thalamic nucleus to the cortex (red). This cortical area then projects from layer 6 reciprocally back to the first order nucleus (light green). Each area is also non-reciprocally connected to a higher order thalamic nucleus. The layer 5 input to the thalamus (dark green) is an "efference copy" of the layer 5 output to the motor system in the brainstem and spinal cord. This copy is forwarded to a higher cortical area (blue). Direct cortico-cortical connections are also depicted between cortical layers and cortical areas (pale gray lines). CP, cerebral peduncle; FO, first order thalamic nuclei; GP, globus pallidus; HO, higher order thalamic nuclei; ic, internal capsule; RTN, reticular thalamic nuclei; SP, subplate; Str, striatum; S1, primary somatosensory cortex; S2, secondary association somatosensory cortex; Po, posterior thalamic nuclei; VPM, ventral posteromedial nucleus; wm, white matter. Adapted from Grant et al, 2012.

1.4.2. Driver and modulator inputs

The anatomical and physiological properties of corticothalamic axons and their synapses differ markedly from each other enabling us to identify them based on their distinct characteristics (Usrey and Sherman, 2018). Layer V projection neurons provide the so-called feedforward ‘driver inputs’ to the HO thalamic nuclei. These driver inputs are characterized by their large synaptic boutons formed on proximal dendrites of thalamic relay cells, often on several sites of the same dendrite. Stimulation of these terminals evokes fast and large excitatory postsynaptic potentials (EPSPs), showing paired-pulse depression and transmission through ionotropic postsynaptic receptors, mainly α-amino-3-hydroxy-5-methy-4- isoxazolepropionic acid (AMPA) and N-methyl-D-aspartate (NMDA) (Sherman and Guillery, 2013; Sherman, 2016; Reichova and Sherman, 2004). Driver input with the similar characteristics is also provided to FO thalamic nuclei from afferents originating from the sensory periphery (Sherman and Guillery, 1996). On the other hand, layer VI feedback inputs projecting to all thalamic nuclei are called ‘modulator inputs’ with their synapses occupying roughly 40-50% of the total contacts formed onto relay cells in thalamic nuclei. These are characterised by their small synaptic boutons located on single sites of distal dendrites of relay cells. Stimulation of these terminals evokes slow and small graded EPSPs, demonstrating paired-pulse facilitation and transmission through both ionotropic (AMPA and NMDA) and metabotropic glutamate receptor mGluR1 receptors (Sherman and Guillery, 1996; Reichova and Sherman, 2004; Usrey and Sherman, 2018). Layer VIb projections to higher order thalamic nuclei are small, they do not provide collaterals to thalamic reticular nucleus and they have specificity according to their cortical origin (Hoerder-Suabedissen et al, 2018).

1.5. Visual system development

In this study, I focussed on the mouse visual system in order to investigate the development and plasticity of the corticothalamic circuit.

In the visual system, information is first processed in the thalamus with inputs relayed to the visual cortex and subsequently conveyed through projections to extra-striate hierarchical organized areas characterized by unique anatomical and functional features in order to process different subsets of stimuli (Homman-Ludiye and Bourne, 2014; Rosa and Krubitzer, 1999). The dLGN, the primary relay of visual inputs to the cortex, receives “driver” projections from the retina and “modulator” projections from layer VI of primary visual cortex (V1). These different projections innervate thalamic relay neurons in a highly coordinated manner encoding for receptive fields, which then combine into more complicated features in the cortex. Cortico-cortical communication and the timing of corticogeniculate innervation are regulated over the first postnatal week through distinct molecular guidance cues (Sherman and Guillery, 2002; Sherman and Guillery, 2006; Brooks et al, 2013; Chou et al, 2013; Piscopo et al, 2013; Seabrook et al, 2013; Thompson et al, 2016). Retinal projections have another main target, the superior colliculus (SC), a midbrain retinorecipient structure, where they densely innervate its superficial layer to control eye movements. This structure operates more like a retinal driver rather than a non-retinal modulator (Godement et al, 1984; Ackman et al, 2012; Bickford et al, 2015).

The majority of retinal ganglion cell (RGC) axons originating from the nasal and temporal retina (95%), cross the optic chiasm by E13.5 to reach the contralateral hemisphere from E16.5-P0, with their terminals occupying ~90% of the total dLGN area. These axons reach the superior colliculus at E18.5. The remaining RGC axons arising from the ventro-temporal part of the retina, project directly to the ipsilateral dLGN without crossing the optic chiasm, and reach dLGN later at P0-P2. These axons occupy only 10% of total dLGN and are located in its dorso-medial region. Upon their arrival, ipsilateral and contralateral axons largely overlap; however, at P4, the axons gradually retract and eventually refine into non-overlapping regions by natural eye opening (~P12), when visually evoked activity begins (Pfeiffenberger et al, 2005; Huberman et al, 2008; Bickford et al, 2010; Wilks et al, 2013).

In mice, retinogeniculate input originates from collateral axons arising from a subset of retinocollicular afferents (Ackman et al, 2012). Although retinal input to dLGN contributes only to 5-10% of synaptic formation, it nevertheless provides the primary excitatory drive for TC relay cells. The remaining synapses are generated from non-retinal projections arising from layer VI of visual cortex, TRN and brainstem nuclei (Sherman and Guillery, 1998; Bickford et al, 2010). With eye-specific segregation and synaptic formation occurring during the second postnatal week, it was first demonstrated that the input is refined resulting in the innervation of 1-3 RGCs in each thalamic relay cell (Godement et al, 1984; Jaubert-Miazza et al, 2005). However, recent studies employing novel genetic techniques, such as genetic labelling of specific RGC populations and retrograde tracing of single dLGN cells from V1, have shown that different modes of visual integration exist with some relay cells receiving inputs from 1-2 RGCs and others from 12-30 RGCs (Cruz-Martin, 2014; Dhande et al, 2015; Morgan et al, 2016; Litvina and Chen, 2017; Rompani et al, 2017).

Retinal axon receptive fields are organized inside the dLGN based on the eye of origin, retinal topography and RGC type (Guido, 2018). The topographic organization of the RGC axons to their target is called eye-specific segregation and is crucial for the proper organization of binocular vision (Rebsam et al, 2012). This specific retinotopy observed in the RGC axon organization is regulated by gradients of molecular guidance cues, mainly by the Eph family. Eph-A receptor tyrosine kinases and their cell surface-bound ligands, ephrin-As, play an important role in the guidance of RGC axons and the establishment of eye-specific topographic maps in dGLN with the most studied molecule of this family being EphA5 (Vanderhaegen et al, 2000; Ellsworth et al, 2005; Huberman et al, 2005; Pfeiffenberger et al, 2005).

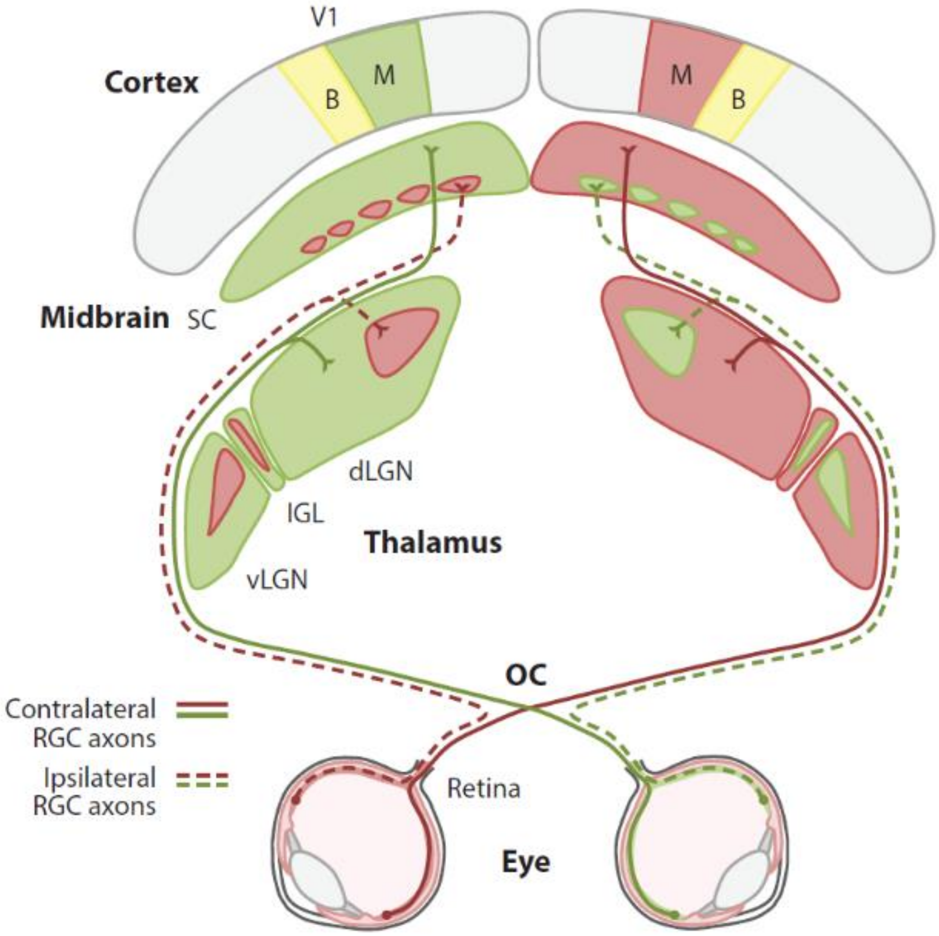

Figure 1.5: Development of retinal axons. Axonal projections from the two eyes are segregated into distinct domains within some retinorecipient targets that receive binocular input. dLGN neurons send their axons to V1, which in mouse is composed of two zones. The monocular zone (M) receives information via dLGN exclusively from the contralateral eye, whereas the binocular zone (B) gets input from both eyes. Other abbreviations: dLGN, dorsal lateral geniculate nucleus; IGL, intergeniculate nucleus; OC, optic chiasm; RGC, retinal ganglion cell; SC, superior colliculus; V1, primary visual cortex; vLGN, ventral lateral geniculate nucleus. Adapted from Seabrook et al, 2017.

1.5.1. The role of spontaneous activity in the development of the visual system

In the retina, prior to eye opening, intrinsic activity in the form of spontaneous waves is present before visual experience occurs. Retinal axons have mature synapses that can transmit spontaneous waves from the retina to the dLGN at birth (Mooney et al, 1996; Ackman et al, 2012). There are three forms of spontaneous waves; embryonic stage I calcium waves mediated by gap junctions, the stage II waves propagating from P0 and mediated by cholinergic transmission, and stage III waves propagating from P10 and mediated by glutamatergic transmission (Feller et al, 1996; Syed et al, 2004; Firth et al, 2005; Ackman et al, 2012). It has been shown that this spontaneous activity includes spatial and temporal information essential for the refinement of visual pathways (Ackman et al, 2012). Moreover, spontaneous calcium waves have been associated with the regulation of the speed of TCA sprouting. This activity-dependent process is mediated by receptors such as DCC and Robo1 (Mire et al, 2012; Castillo-Paterna et al, 2015).

Various manipulations of spontaneous waves have been employed in the past for unravelling the role of retinal waves in the development of the visual circuits. Blockage of spontaneous waves by TTX intraocular injections in cats (Shatz and Stryker, 1988) as well as epibatidine administration in ferrets (Penn et al, 1998) inhibited their propagation, and thus disturbed eye-specific segregation. Furthermore, epibatidine treatment in ferrets used to prevent stage II spontaneous waves, resulted in the severe impairment of ODC pattering and the increase of receptive field size in the visual cortex (Huberman et al, 2006). These results indicate the necessity of spontaneous retinal activity for the proper eye-specific segregation and ODC formation.

Finally, microarray data by Majdan and Shatz (2006) obtained from the visual cortex of mice after monocular enucleation in various developmental stages revealed a plethora of genes that were downregulated at all ages. These included the brain-derived neurotropic factor (BDNF), the early growth factors (Egr) 1 and 2 and transcription factor Fos. Also, many genes identified are regulated in the MAPK signaling pathway, indicating its implication in the regulation of the visual circuit formation (Majdan and Shatz, 2006). What is more, binocular enucleation experiments in mice showed a downregulation in the expression of ephrinA5 in the enucleated dLGN (Dye et al, 2012). Genetic ablation of RGCs also showed the differential expression of Adamts metalloproteinases in the deprived dLGN, proposing the role of retinal activity in the gene expression of dLGN (Brooks et al, 2013).

1.5.2. The role of experience in the development of the mouse visual system

Eye-specific segregation is evident not only in the dLGN, but also in V1. The classic experiments of Hubel and Wiesel (1963) and their following studies revealed the existence of functionally defined columns, called ocular dominance columns (ODCs). Within an ODC, a column of cortex responds preferentially to a particular orientation of visual stimuli across V1 (Hubel and Wiesel, 1963; Hubel and Wiesel, 1968; Hubel and Wiesel, 1977; Hubel et al., 1977). These ODCs are a well-established model for examining the role of early visual experience in cortical plasticity (Katz and Crowley, 2002). Invasive experiments, including eyelid suturing (Gordon and Stryker, 1996), intraocular tetrodotoxin (TTX) injections (Frenkel and Beer, 2004), slitting of the optic chiasm (Berlucci and Rizzolatti, 1968) as well as monocular and binocular enucleations (Toldi et al, 1994; Toldi et al, 1996; Negyessy et al, 2000), and non-invasive retinal manipulations, such as eye patching (Zapasnik and Burnat, 2013), dark rearing from birth (Morales et al, 2002; Kreczko et al, 2009; Yang et al, 2013), dark or light exposure with different dark-light periods (Blakemore and Cooper, 1970; He et al, 2006; Guo et al, 2012; Petrus et al, 2014), have been widely used for investigating the role of experience in the development of the visual system. Using these methods, researchers were able to characterize the ocular dominance plasticity occurring during the critical period, a particularly sensitive phase of development lasting from P20-P35, during which alterations in visual experience change significantly the ODCs in V1 (Gordon and Stryker, 1996; Sur et al, 2013). Monocular deprivation during the critical period resulted in decreased response from the deprived eye and increased response from the remaining one to the cortex. These changes are accompanied by altered TCA connectivity with TCAs from the deprived eye to be eliminated and the ones coming from the remaining one to be expanded (Shatz and Stryker, 1978; Antonini and Stryker, 1996). What is more, this deprivation during the critical period induces changes in the distinct transcriptional profile observed in this period, activating genes related to neuronal degeneration and growth factors (Lyckman et al, 2008).

1.6. Neuroplasticity

Sensory systems are represented in the primary sensory areas of the brain in remarkably precise and refined wired maps. During embryogenesis, sensory cortices are topographically and morphologically established independently of external stimuli and mediated by molecular factors. However, later in gestation their size and position vary depending on peripheral stimuli, exhibiting their “plastic” capacity (Huberman et al, 2008; Thompson et al, 2016). This plastic nature of the brain has been demonstrated in various systems in which, upon peripheral deprivation such as deafness or blindness, processing of inputs was increased to the remaining modalities as a compensatory mechanism to the loss of the other sense. This phenomenon is known as cross-modal neuroplasticity. This plasticity was detected in the visual cortex following visual deprivation, where it has been suggested to arise through enhancement of cortical intermodal connections, unmasking of already existent cortical connections or sprouting of novel cortical connections (Bavelier and Neville, 2002; Pascual-Leone et al, 2005).

1.6.1. Experience-dependent cross-modal plasticity

Sensory experience has been proven to be essential for the modification of structural and functional connectivity in the cortex. Cross-modal plasticity appears after early or late onset of blindness with visual cortex becoming activated by auditory or somatosensory stimuli in visually deprived animal models after enucleation at birth or congenital blindness (Toldi et al, 1994; Rauschecker, 1995; Toldi et al, 1996; Yaka et al, 1999; Negyessy et al, 2000; Bronchti et al, 2002; Izraeli et al, 2002; Piché et al, 2007; Chabot et al, 2007). Charbonneau *et al* (2012) provided evidence of direct projections from auditory and somatosensory cortices to V1 in visually deprived mice, both congenitally anophthalmic and perinatally enucleated (Chabornneau et al, 2012). What is more, auditory stimuli were found to activate the occipital cortex and dLGN, the major forebrain visual targets, in the blind mole rat (Bronchti et al, 1989). Laramée *et al* (2013b) also revealed an essential disorganization of projections from V1 to corpus callosum and extrastriate areas using the same animal models, highlighting the necessity of retinal input for the establishment of cortico-cortical circuit (Laramée et al, 2013b).

Cross-modal plasticity has also been investigated at the level of the thalamus. Experiments in young ferrets in which the cochlea and inferior colliculus were removed, have revealed a rerouting of retinal fibres to project to the MGN in addition to the dLGN, with visual information been indirectly conveyed to A1 (Sur et al, 1988; Roe et al, 1992; Angelucci et al., 1997; Angelucci et al., 1998). A later microarray analysis showed that the rewired MGN had a transcriptional profile similar to the control dLGN, indicating that peripheral input might determine FO gene expression in a modality-specific manner (Horng et al, 2009). Furthermore, in adult congenitally blind mice, ascending somatosensory projections have been demonstrated to prominently innervate and arborize into dLGN (Asanuma and Stanfield, 1990). Similar effect has also been shown in HO thalamic nuclei with input from somatosensory cortex being rewired to the visual HO LP after binocular enucleation (Mooney and Rhoades, 1983).

1.6.2. Experience-independent cross-modal plasticity

Although a plethora of studies identified the experience-dependent mechanism that drives cross-modal plasticity, the early adaptations found before the onset of sensory experience could not be explained.

As previously mentioned, binocular enucleation of mice at birth alters the expression patterns of genes involved in the establishment of cortical maps at P10, a timing when sensory experience has not yet started (Dye et al, 2012). Subsequent experiments of neonatal enucleations in rats resulted in increased barrel size, indicating cross-modal plasticity between visual and somatosensory systems before active sensory whisking occurs (Fetter-Pruneda et al, 2013; Abbott et al, 2015). These experience-independent mechanisms of cross-modal plasticity might be induced by spontaneous activity through changes in the propagation of retinal waves as it has been demonstrated that they are involved in the regulation of cortical arealization before the onset of sensory experience (Huberman et al, 2006; Espinosa and Stryker, 2012). Recent studies from Moreno-Juan et al (2017) have demonstrated that when visual input is removed embryonically, this leads to changes in gene expression and TCA sprouting, which highly reorganize the somatosensory cortex as early as P4. The same results were also shown following silencing of thalamic spontaneous retinal waves, which induced alterations in the size of primary cortical areas during development prior to sensory experience (Moreno-Juan et al, 2017). Therefore, it is possible that the cross-modal plasticity demonstrated in this study was due to changes in the developmental timing of sensory systems controlled by the spontaneous activity, and not due to the experience-dependent activity.

1.6.3. Cross-hierarchical plasticity

As indicated from the studies mentioned in sections 1.6.1. and 1.6.2., the main focus of research in the past years was the unravelling of the mechanisms that regulate neuronal plasticity within different modalities. However, the cross-hierarchical plasticity, meaning the plasticity between FO and HO thalamic nuclei and their targets, has been largely neglected.

In the absence of FO thalamic input, primary cortices acquire transcriptional characteristics of associative secondary cortical areas, indicating the importance of thalamic input in the development and determination of primary cortical identity (Pouchelon et al, 2014; Chou et al, 2013; Vue et al, 2013). Interestingly, previous work by Pouchelon et al (2014) has demonstrated rewiring of TCAs from the Po to Layer IV of S1 after genetic ablation of the VPM with deprived S1 circuits acquiring S2-like properties (Pouchelon et al, 2014). Moreover, recent publication by using monocular enucleation at birth, showed that loss of retinal input results in premature innervation of layer V and VI projections ingrowth to the dLGN (Grant et al, 2016). Additionally, layer V corticothalamic axons rearrange and arborize aberrantly inside the FO dLGN after visual deprivation with branches forming synapses at P8. These effects were also observed after blockage of spontaneous retinal waves with epibatidine in Layer VI labellled transgenic mice (Golli-*tau*-eGFP), indicating that intrinsic activity might also be involved in the establishment of FO- or HO-like thalamic identity (Grant et al, 2016). These two publications are the first evidence of cross-hierarchical rewiring of thalamocortical and corticothalamic projections respectively, following sensory deprivation.

Early layer VI axonal innervation to dLGN was previously described by Seabrook et al (2013), where retinal input was abolished either surgically at birth with binocular enucleation or genetically with *math5-/-* mutant mouse line (Seabrook et al, 2013). What is more, using the same models of retinogeniculate axon depletion, Brooks et al (2013) described a temporal regulation of the innervation of layer VI corticothalamic axons to dLGN controlled by aggrecan, indicating the role of guidance cues in the regulation of corticothalamic ingrowth (Brooks et al, 2013).

Later studies in the somatosensory and visual system revealed that peripheral input contributes to the establishment of transcriptional identity of the thalamic nuclei to which it projects. Frangeul and colleagues ablated at birth sensory input to the VPM by performing infraorbital nerve section (IONS) as well as retinal input to the dLGN by bilateral enucleation, and demonstrated that the FO thalamic nuclei lacking peripheral input have a gene expression profile similar to that of HO nuclei, suggesting that HO gene expression is a default state from which FO identity emerges in an input-dependent manner (Bishop, 1959; Butler 2008; Frangeul et al, 2016). It was also previously demonstrated that lack of retinal input achieved by bilateral optic nerve section at P0 directly affected migration of dLGN interneurons at P20, indicating the importance of peripheral input in the incorporation of interneurons into the dLGN (Golding et al, 2014). In the same study, the authors also showed that spontaneous activity affects dLGN interneuron migration by blocking spontaneous waves with TTX, which dramatically decreased the interneuron migration speed in dLGN (Golding et al, 2014).

Overall, all the aforementioned studies imply the different levels by which sensory systems are developed and functionally regulated. Understanding the plastic changes following input deprivation has been focused mainly on the peripheral afferents to the subcortical structures and mostly in the thalamus as well as in the mechanisms by which thalamic axons target specific cortical areas. However, corticothalamic projections and the mechanisms mediating their development and plasticity remain largely unknown.

1.7. Aims of thesis

The main aim of this thesis was to examine the mechanisms underlying corticothalamic plasticity in the mouse visual system following sensory deprivation by monocular enucleation. More specifically, my aims were:

1. To identify the origin of corticothalamic projections to the dLGN after monocular enucleation. For this purpose, I employed viral tracing of layer V projections from V1 and S1 to the thalamus of control and enucleated mice in order to investigate the ingrowth of layer V fibres into the dLGN and LP and the potential of cross-modal plasticity after visual deprivation.

2. To characterize the anatomy of the layer V formed synapses after MoE in the deprived dLGN. For this, the size and density of synaptic boutons were assessed by immunohistochemistry to address whether the properties of the synapses are altered by the lack of retinal input.

3. To validate the expression of selected genes from previous microarray performed in our laboratory, in which differential gene expression was observed in deprived dLGN compared to control. To accomplish this, I performed *in situ* hybridization experiments to examine the expression pattern of genes in the deprived dLGN.

2. Materials and Methods

2.1. Transgenic Mice

All experiments on transgenic animals were in accordance with the UK Home Office regulations and the local ethical review. Procedures were performed under valid Animals (Scientific Procedures) Act personal and project licences in the Biomedical Sciences Building, University of Oxford, UK.

The transgenic line used for this research was the Cre-recombinase expressing strain Tg(Rbp4-cre)KL100Gsat/Mmucd (*Rbp4-Cre*; Jackson Laboratories), which can be used to label a subset of cortical layer V neurons and axons (Grant et al, 2016), crossed with the tdTomato reporter line B6;129S6-Gt(ROSA)26Sortm14(CAG-tdTomato)Hze/J (*Ai14*) for labelling of layer V neurons.

2.2. Monocular Enucleation (MoE)

In order to investigate the role of retinal input in the development of corticothalamic projections, I performed monocular enucleation on Rbp4-Cre::tdTomato pups at birth to assess the effect of visual deprivation on the ingrowth of corticofugal layer V projections to visual thalamic nuclei (dLGN and LP). P0 Rbp4-Cre pups were anaethetized by hypothermia on ice until unresponsive. The surrounding area of the left eye was sterilized with povidone-iodine and a small incision was performed on the eyelid using a 5mm microsurgical scalpel. Following, the incision was opened using sharp forceps for better visualization of the area and the entire left eye (retina, retinal pigmented epithelium and lens) was removed by cutting the optic nerve with the forceps. After the procedure, the animals were warmed in a heating chamber until their skin colour and normal movement recovered, and then returned to the home cage.

2.3. Unilateral Viral Injections for Axon Tracing

To trace the axonal projections of layer V cells to subcortical targets, especially to thalamus and superior colliculus, in Rbp4-Cre::tdTomato control and monocularly enucleated mice at P0, we performed unilateral viral injections of a Cre-independent GFP adeno-associated virus (AAV) targeting cortical layer V. The use of a non-Cre dependent virus was unintentional as I was originally planning to use a Cre-dependent virus for my experiment in order to trace specifically layer V corticofugal axons. However, instead of this, the Cre-independent virus stated above was wrongly delivered and this mistake was only noticed after completion of all the injections for this study. Adult mice (age range 8-10 weeks) were deeply anaesthetized with isoflurane and placed in a stereotaxic frame. After midline skin incision, a unilateral craniotomy was performed over V1 or S1 (see table below for coordinates). Using a calibrated glass micropipette, mice were injected into the right hemisphere with either 100nL of AAV2-CAGGS-Arch-GFP (University of North Carolina Vector Core, Ed Boyden repository) Cre independent virus in monocular sector of V1 (V1M; n=3 for each condition), or 200nL of the same virus in the barrel field area of S1 (n=3 for MoE animals). Injection was over the course of 1min, and micropipette was left in place for another 5min to reduce reflux of virus. After retraction of the micropipette, the skin was sutured and animals were allowed to recover in a heated recovery chamber, before being returned to their home cage. Appropriate analgesia was provided during and after the surgery. We chose to inject the right hemisphere of the mice as we enucleated their left eye thus depriving of retinal input the right hemisphere. At 3-4 weeks after the surgery, when GFP was expressed, mice were perfused.

Rbp4-Cre::tdTom mouse line	Region	Bregma (mm)	Laterality (mm)	Depth (mm)	Volume	Number of animals
Control (no MoE)	V1M	3.4 caudal	2.1 right	0.5	100nL	3
MoE	V1M	3.4 caudal	2.1 right	0.5	100nL	3
MoE	S1	1.5 caudal	2.7-3.0 right	0.8	200nL	3

Table 1: Coordinates of injection sites of Cre-independent GFP virus in control and MoE Rbp4-Cre::tdTomato mice, volume injected and number of animals used from injections on each cortical area.

2.4. Tissue Collection

For immunohistochemistry experiments, adult mice were anaethetized by intraperitoneal injection with pentobarbitone (150 mg/kg, Pentoject, Animal Care Ltd, UK) and perfused transcardially with 0.1M phosphate buffered saline (PBS, pH7.4) followed by 4% paraformaldehyde solution (PFA; Sigma-Aldrich F8775) in 0.1M PBS. Brains were then dissected out of the skull and post-fixed in 4% PFA overnight. The collected tissue was stored in 0.1% sodium-azide in 0.1M PBS. For sectioning, tissue was embedded in 5% agarose (Bioline) in 0.1M PBS and cut to 50μm sections in the coronal plane on a vibrating microtome (Leica VT1000S).

For *in situ* hybridization experiments, P6 and P8 mice were killed by cervical dislocation and brains were dissected out in RNAse-free conditions. Dissected brains were embedded in O.C.T compound (Tissue Tek) on dry ice and stored at –80°C. The tissue was sectioned coronally to 20μm on a cryostat (Leica, Jung CM3000) and mounted on 1.0mm SuperFrost Ultra Plus slides (Thermo Scientific^{TM})

2.5. Immunohistochemistry

For synaptic labelling of layer V fibres in thalamic nuclei, immunostaining against Vesicular Glutamate Transporter 1 (VGluT1) was performed on 50μm coronal dLGN-containing free-floating sections of adult fixed Rbp4-Cre::tdTomato brains. Sections were blocked with 0.1% Triton-X100 (Sigma-Aldrich) and 2% donkey serum (Sigma Aldrich) in 0.1M PBS for 2 hours at room temperature (RT) on a rocking platform. Sections were then incubated with the primary antibody guinea-pig anti VGluT1 (Chemicon, AB5905, 1:10000) in blocking solution for at least two days at 4°C on a rocking platform. Sections were subsequently incubated with donkey anti-guinea-pig biotinylated secondary antibody (Jackson ImmunoResearch, 706-065-148, 1:100) in blocking solution for 2 hours at RT and then with Cy5 streptavidin-conjugated fluorophore (Invitrogen, SA1011, 1:200) in blocking solution for 2 hours at RT. Finally, they were counterstained with 4′,6-diamidino-2-phenylindole (DAPI; Invitrogen, D3571, 5μm/mL) and mounted in PBS.

2.6. *In situ* hybridization probe synthesis

Riboprobes for Otx2, Kcnk9, EphA5, Calb2 and Cbln2 were synthesized using the first strand cDNA synthesized from RNA extracted from thalamus and cortex of mouse samples. The forward and reverse primers for each gene (Table 2) were used for the generation of gene-specific fragments by polymerase chain reaction (PCR). The PCR products were subsequently ligated with T4 DNA ligase into the blunt cloning vector pSTBlue-1 (Novagen). NovaBlue single competent cells (Novagen) were transformed with the ligated product, and the plasmid was then isolated using QIAprep Spin Miniprep Kit (Qiagen). After sequencing, the plasmid DNA was purified using the QIAquick PCR Purification Kit (Qiagen). Finally, the antisense and sense (negative control) RNA probes were labelled with digoxigenin-UTP (DIG) RNA labelling mix (Roche) by T7 and SP6 RNA polymerase, respectively. Final riboprobes were diluted and stored at -20°C.

Calb2 forward primer: *5'-GATGCTGACGGAAATGGG*

Calb2 reverse primer: *5'-CCCTACCAGCCACCCTCT*

Cbln2 forward primer: *5'-CAGCTTCCACGTGGTCAA*

Cbln2 reverse primer: *5'-AGCCCCCAGCATGAAAAC*

Primer sequences for Otx2, Kcnk9 and EphA5 probes were not available by Dr Shuichi Hayashi, who provided us with these probes.

2.7. *In situ* Hybridization

In order to examine the expression pattern of the molecules selected from the microarray and qPCR analysis in control and deprived dLGN, *in situ* hybridization was performed in RNA-free conditions in cryosectioned samples following a 3-day protocol. An n=3 individual experiments was performed for each probe in tissue from control and enucleated mice at P8. All the solutions made for this experiment were diluted in distilled autoclaved water containing 1% diethyl pyrocarbonate (DEPC; Sigma-Aldrich) to avoid RNAse contamination. The first day, cryosections were fixed in 4% PFA for 10 minutes and acetylated with triethanolamine hydrochloride and acetic anhydride, followed by washes in PBS. Digoxigenin (DIG) labelled RNA probes against *Otx2* (500ng), *Kcnk9* (500ng), *EphA5* (400ng), *Calb2* (500ng), and *Cbln2* (600ng), were diluted in hybridization buffer [(50% formamide, 10mM Tris (pH 7.6), 200μg/mL *Escherichia coli* transfer RNA, 1× Denhardt's solution, 10% dextran sulfate, 600mM NaCl, 0.25% sodium dodecyl sulfate (SDS), 1mM ethylenediaminetetraacetic acid (EDTA)] and applied on the sections for overnight incubation at 70°C in a humidified chamber. Otx2, Kcnk9 and EphA5 probes were kindly provided by Dr Shuichi Hayashi. The following day, sections were placed in 5x saline sodium citrate (SSC) in a 70°C waterbath for 5 minutes and then incubated in 0.2x SSC at 70°C in the heating chamber for at least 1h. All subsequent washing steps were performed in TBS [100mM NaCl, 100mM Tris-Cl (pH7.5)]. Sections were incubated firstly with 0.5% Boehringer Blocking Reagent (Roche) in TBS for at least 1h at RT and secondly with an alkaline phosphatase (AP) anti-DIG antibody (Roche, 1:2000 in blocking solution) at 4°C overnight. The third day, sections were washed with NTM [100 mM Tris (pH 9.5), 100 mM NaCl, 50 mM MgCl2] prestaining buffer and then incubated at 4°C with a staining buffer containing NBT (Nitro Blue Tetrazolium)/ BCIP (5-bromo-4-chloro-3-indolyl-phosphate) (Roche) in humidified chamber and monitored for the next 16-48 hours, depending on each probe, for development of the desired colour reaction. For fluorescent colour reaction, the FastRed TR/Naphthol AS-MX Tablets (Sigma-Aldrich) were used for detection of the AP anti-DIG antibody. 1x Tris (pH8.2) was used as a prestaining buffer and for the dilution of the tablets. Incubation with the fast red staining buffer lasted overnight at 4°C. The next day sections were counterstained with DAPI and mounted in FluorSave (Millipore).

2.8. Image Acquisition and Processing

Fluorescent and bright field microscope images were obtained using a Leica epifluorescence microscope (DMR) with a Leica DC500 CCD camera. Confocal images for viral tracing experiments were acquired using a Zeiss LSM 710 laser scanning confocal microscope. For imaging of the fast red staining of the *in situ* hybridization slides, images were acquired using an Inverted Confocal Microscope Olympus FV1200.

Images were contrast adjusted on ImageJ software. Figures included in Section 3 were constructed using Adobe Photoshop CS6 and Adobe Illustrator CS6 after microscopic analysis of at least three sections from three individuals ($n_{experiments}$ =3).

2.9. Data Analysis

For analysing the imaging data acquired, all images were brightness and contrast adjusted, their background was substracted and they were auto-thresholded by using the respective plugins on ImageJ software.

For measurement of the thickness of the tdTom+ dorsal axon bundle, the length of the bundle on the dorsal part of dLGN was quantified using ImageJ. Co-localization of the tdTomato+ and VGluT1+ boutons formed in control and enucleated dLGN was quantified from confocal stack images of the upper lateral part of dLGN (n=3 brains, at least 3 medial sections per brain were measured).

For the comparison of control and enucleated dLGN size in the same brain, analysis was done by using a two-tailed, paired, non-parametric Wilcoxon Student's t-test. For comparing the bouton density in the dLGN of control and enucleated virally injected brains (n=3 per condition), a two-tailed, unpaired, non-parametric Mann-Whitney Student's t-test was performed.

For the measurement of the density of Otx2, Kcnk9, Calb2, Cbln2 and EphrinA5 positive cells in control and enucleated dLGN in the same brain, colocalization of DAPI+ and FastRed+ cells in the whole dLGN was quantified (n=3 experiments, 3 medial sections per brain were measured). For comparison of the density of positive cells for each gene in control and enucleated dLGN, a two-tailed, paired, non-parametric Wilcoxon Student's t-test was performed.

Statistical analysis and graph generation were performed on GraphPad Prism 8. Differences were considered significant when $P < 0.05$.

3. Results

3.1. Rewiring and origin of Layer V corticothalamic projections to dLGN following retinal input deprivation

Corticothalamic projections originate from layers V and VI of the neocortex and vastly outnumber by 1:10 the ascending afferents in all sensory thalamic nuclei (Jones, 2007). Corticofugal projections to the thalamus are comprised of two anatomically distinct projection systems; a feedforward system that emanates from layer V with projections forming large, proximal synapses to HO thalamic nuclei, and a feedback system arising through layer VI projections with small synaptic terminals on distal dendrites in both FO and HO nuclei (Sherman and Guillery, 2002; Deschênes et al, 1994; Rouiller and Welker, 1991). In the visual system, projections from layer V neurons innervate the vLGN, superior colliculus and OPN, whereas layer VI neurons project to the dLGN and LP, with projections from dLGN reaching the visual cortex directly (Schmidt et al, 1993; Seabrook et al, 2013). However, it still remains unknown whether these inputs are required for proper targeting of RGC axons and receptive field properties during development of the visual system connectivity.

In order to study the role of retinal input in the ingrowth of corticothalamic fibres to dLGN as well as the plastic changes occurring in the visual thalamic nuclei, the first-order dLGN and the higher-order LP, we performed monocular enucleation (MoE) at P0 to Rbp4-Cre::tdTomato mice, a mouse line which enables the assessment of layer V fiber ingrowth to subcortical areas. Monocular enucleation is a drastic model for visual deprivation as, in contrast with the frequently used monocular deprivation paradigms, such as eye patching or lid suturing, it eliminates irreversibly all retinal activity from the removed eye, including light-driven patterns and spontaneous waves. This model also allows intra-animal control, preventing variability within the litter in contrast with the binocular enucleation approaches. What is more, with enucleation, complete abolishment of inhibitory binocular interactions is achieved and gene expression in the visual system is significantly altered (Madjan and Shatz, 2006). When MoE is performed at birth, it elicits robust structural rearrangements and synaptic changes along thalamocortical, intracortical and subcortical circuits, especially in the hemisphere contralateral to the removed eye (Nys et al, 2015; Toldi et al, 1996). Only 5-15% of retinal input eventually reaches the dLGN through the expanded ipsilateral fibres. This effect establishes MoE as a valuable model to investigate the role of sensory input to the thalamus on the development of corticothalamic projections (Ackman et al, 2012).

Throughout this chapter, I will use the term ‘enucleated’ to refer to the contralateral hemisphere to the removed eye, which is deprived of 85-95% of retinal input after monocular enucleation, only receiving the remaining input from the ipsilateral eye (Valverde, 1968; Godement et al., 1980; Jaubert-Miazza et al., 2005).

3.1.1. Layer V fibres rearrange and form synapses in the enucleated dLGN

Previous published research by Grant et al (2016) reveled the effect of MoE in Rbp4-Cre::tdTom transgenic mice, where the enucleated dLGN was significantly smaller and axons were rearranged in the dorsal part of the enucleated dLGN forming a thick bundle of fibres at P6 (Grant et al, 2016). In order to correlate with the published literature and confirm whether my MoE model had the same effects in the size and axonal arrangement of the enucleated dLGN in adult mice used for my experiments, thus extending my results into adulthood stage and explore whether the layer V effect previously shown is persistent, I decided to measure the dLGN area size in coronal sections stained with DAPI as well as the thickness of the tdTom+ axon bundle located in the dorsal part of control and enucleated dLGN of the same brain. My results revealed a significant decrease of the size of the enucleated dLGN area compared to the control hemisphere (n=3, p=0.0039, Wilcoxon, two-tailed, paired Student’s t-test) demonstrating an area decrease of 38% (Fig.3.1.1., A-C). As for the axon bundle thickness, my results showed that the axon bundle crossing through the dorsal part of dLGN in the enucleated hemisphere was significantly thicker in comparison with the control (Fig.3.1.1., D-F; n=3, p<0.0001, Mann Whitney, two-tailed, unpaired Student’s t-test), with less axons appearing crossing through the centre of the dLGN, indicating a possible rearrangement of these axons in the dorsal part of the structure.

What is more, I investigated whether these axons are just passing through dLGN or sprout and form synaptic terminals by performing immunostaining against VGluT1, a marker for mature cortically-derived synapses, in order to identify possible tdTom+ VGluT1+ synapses selecting the dorsomedial part of dLGN for the quantification. There was a significant increase of tdTom+ VGluT1+ synapses in the enucleated dLGN in comparison with the control, where very few synapses were found (white arrows showing synaptic boutons in Fig3.1.1. G-I; n=3, p=0.002, Wilcoxon, two-tailed, paired Student’s t-test). This indicated that after enucleation, the axons did not just pass through the FO dLGN, but they sprouted abnormally demonstrating HO-like characteristics, which confirms the cross-hierarchical rewiring effect.

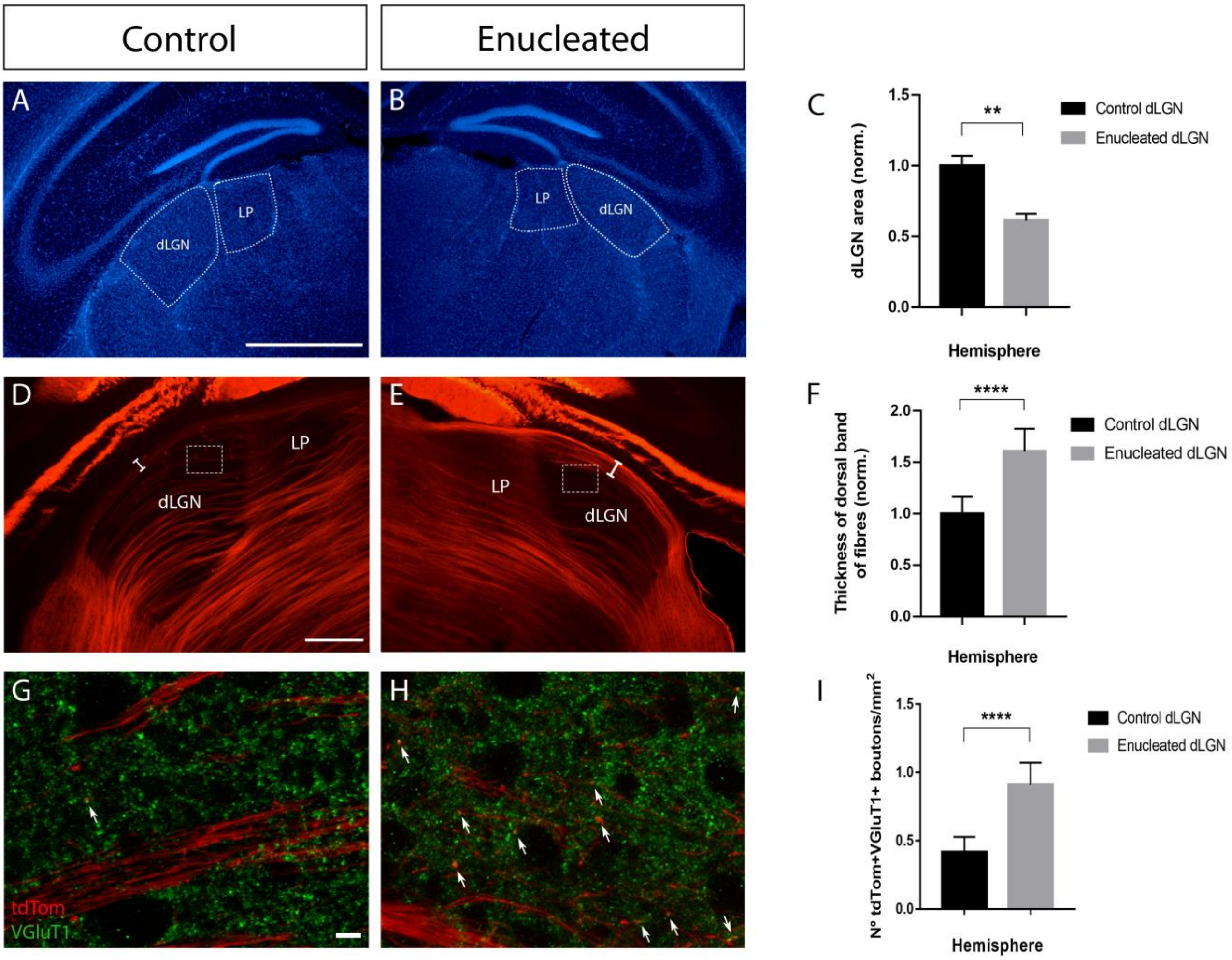

Figure 3.1.1. Changes in dLGN size and Layer V axon innervation and synaptic formation in the dLGN of control and monocularly enucleated Rbp4-Cre::tdTomato adult mice. (A-B) The area of dLGN in mm^2 in coronal sections in control and enucleated adult animals. After enucleation, dLGN appears significantly decreased in size (C) in comparison with the control conditions (area of dLGN and LP demarcated with the dotted white lines)**.** (D) In control dLGN, Layer V axons innervate and pass through the medial part of dLGN with very few axons crossing through the dorsal part (white bracket). (E) Following enucleation at birth, axons exhibit rearrangement inside dLGN, with projections sprouting through the dorsal part of dLGN forming a bundle of fibres (white bracket), that is significantly thicker in the enucleated dLGN (F) in comparison with the control (E). (G-H) High magnification images of the area demarcated by the white boxes in D and E respectively, demonstrating immunostaining against the synaptic marker VGluT1, with synaptic boutons showing a significant increase in the enuceated dLGN compared to the control (I). Results for quantifications based on n=3 animals, at least 3 medial sections per animal. Values shown are mean and standard error. **= significant at p=0.005, ****= significant at p<0.0001. Abbreviations: dLGN, dorsal lateral geniculate nucleus; LP, lateral posterior nucleus; VGluT1, vesicular glutamate transporter 1. Scale bars: 300μm (A-B), 200 μm (D-E), 10 μm (G-H).

3.1.2. Layer V corticofugal fibres to dLGN originate from V1 and not from S1 after monocular enucleation.

As previously mentioned, Grant et al (2016) have demonstrated a cross-hierarchical rewiring of layer V axons in dLGN with projections rearranging in the dorso-lateral part of the dLGN at P6 following monocular enucleation at birth in Rbp4-Cre::tdTom animals. In section 3.1.1, I managed to replicate the effect of enucleation and further extend the data in adult animals of the same mouse line, showing that the rewiring is permanent until adult stages and not temporary in primary developmental stages. However, the cortical source of these rewired layer V projections observed in the deprived dLGN is not known. Therefore, in order to investigate their origin to the dLGN and determine whether there is a cross-modal or intra-modal plastic effect after input deprivation inside dLGN, I decided to perform unilateral cortical injections of an adenoassociated (AAV) Cre-dependent GFP virus in the primary somatosensory (S1) and visual (V1) cortices of Rbp4-Cre::tdTomato adult mice in control conditions and following monocular enucleation at P0. In this manner, I would be able to label the axons only from layer V of each cortical area and follow their ingrowth in the thalamic nuclei. However, due to the issue that occurred with the wrong delivery of the Cre-dependent virus that I was planning to use originally for my experiments to reassure specificity for layer V corticofugal tracing, it is highly possible that in most of the injections performed there was a contamination of other cortical layers, mostly of layer VI, with the virus. For this reason, from the injected brains, I selected for the analysis of the expression pattern of the corticofugal projections to the thalamus only those that were showing a bigger limitation in layer V and/or minimal contamination in layer VI (Fig. 3.1.2., E, G).

My results demonstrated layer V corticofugal axons to the enucleated dLGN originating from V1 and not S1. More specifically, in control conditions, layer V GFP positive projections from S1 innervated the somatosensory first-order VPM and higher-order Po (Fig. 3.1.2., A-B). S1 injections in control conditions were not performed as images were obtained from Allen Mouse Brain Connectivity Atlas (©2011 Allen Institute for Brain Science. Allen Mouse Brain Connectivity Atlas [Internet]. Available from: http://connectivity.brain-map.org/projection/experiment/cortical_map/272735030). In the enucleated animals, the axons from S1 reach the thalamus and innervate again the somatosensory nuclei VPM and Po, completely bypassing the dLGN (Fig. 3.1.2., D). However, the expression of the virus was shown to be higher in VPM and not Po (Fig. 3.1.2., D), as normally expected from layer V projections that reach and sprout in higher-order nuclei. This might be due to contamination of layer VI with the virus in the injection site (Fig. 3.1.2., C) as projections from this layer reach both first-order and higher-order thalamic nuclei. Nevertheless, origin results were not affected as projections from S1 were not found to rearrange to innervate dLGN, which demonstrated that S1 was not the origin of layer V projections after retinal input deprivation.

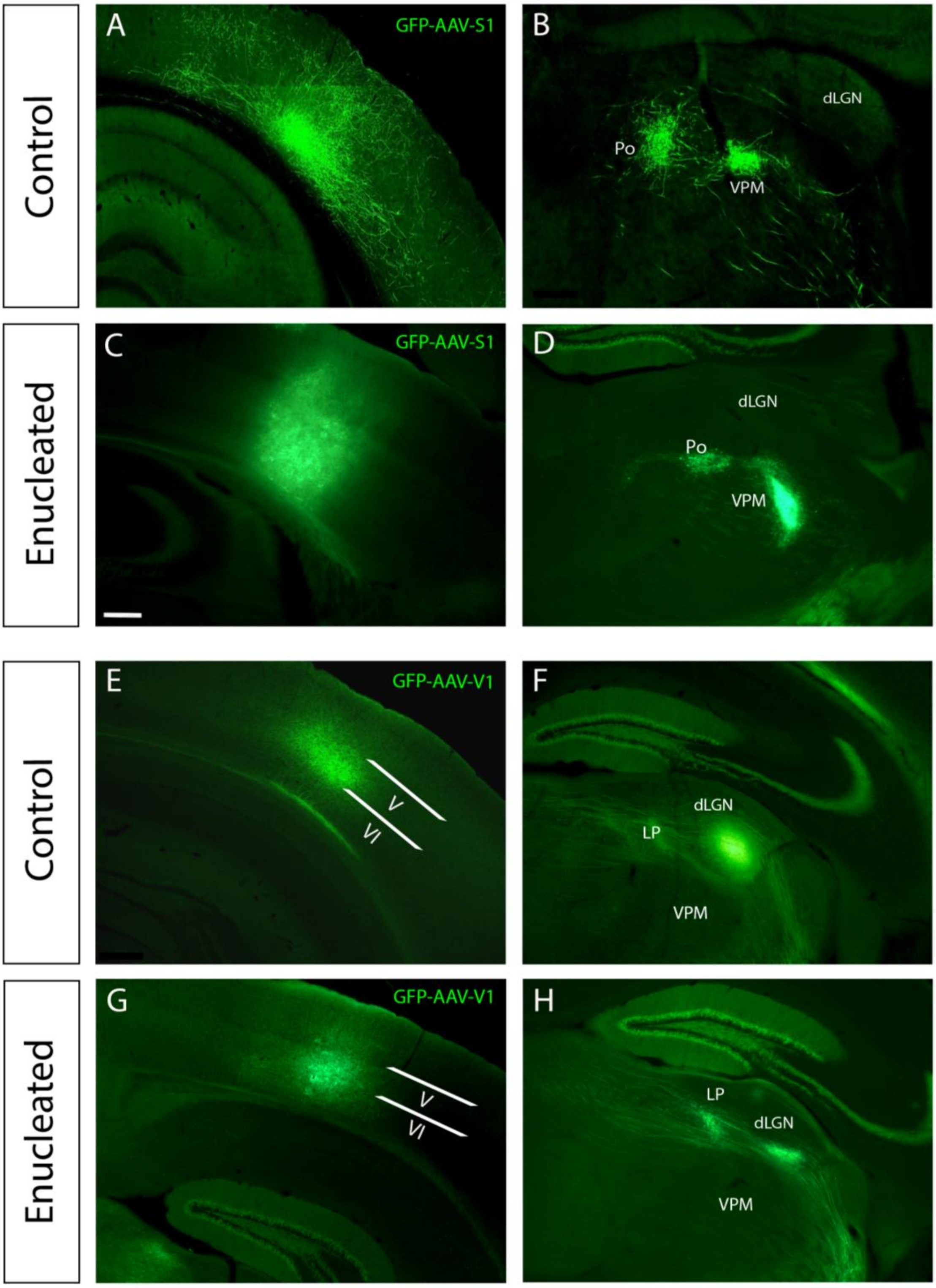

Figure 3.1.2. Layer V corticothalamic axons originate from V1 and not S1 in the dLGN following monocular enucleation at P0 in adult Rbp4::tdTom mice. Coronal sections of cortical S1 and V1 injections with AAV GFP Cre-independent virus in adult mice. (A-B) In control conditions, corticothalamic projections from S1 innervate the somatosensory thalamic nuclei, VPM and Po (images adapted from Allen Institute for Brain Science). (C-D) In mice enucleated at P0, corticothalamic projections follow the same pattern with the control conditions innervating only the VPM and Po and completely bypassing dLGN. (E-F) In control mice, corticothalamic axons from V1 project to the visual thalamic nuclei, dLGN and LP. (G-H) In enucleated mice, axons from V1 innervate dLGN and LP, showing rewiring inside dLGN compared to the control mice, with axons crossing through the lower latero-ventral part of the structure. Abbreviations: AAV, adeno-associated virus; GFP, green fluorescent protein; S1, primary somatosensory cortex; V1, primary visual cortex; VPM, ventral-posteromedial nucleus; Po, posterior thalamic nucleus; dLGN, dorsal lateral geniculate nucleus; LP, lateral posterior nucleus. Scale bars: A-B scale bars unavalaible as images are from publically available Allen Mouse Brain Connectivity Atlas, 200μm (C-H).

On the other hand, layer V GFP positive corticofugal projections from V1 showed innervation in the dLGN and LP both in control and enucleated brains (Fig. 3.1.2., F, H), demonstrating differential pattern of expression in the dLGN in control and input deprivation conditions. More specifically, in control conditions, axons found to pass through the medial part of the dLGN, exhibiting a wide expression through the centre of the structure (Fig. 3.1.2., F). However, in enucleated conditions, GFP positive axons showed a rearrangement, growing through the lower ventro-lateral part of the deprived dLGN (Fig. 3.1.2., H). In both cases, axons passed through dLGN and eventually reached LP, and more specifically LPLR, as expected, showing no difference in the pattern of expression inside this structure (Fig.3.1.2., F, H).

3.1.3. The density of Layer V formed synapses was increased in the enucleated dLGN.

Cross-hierarchical rewiring in the dLGN after input deprivation was firstly identified in our laboratory by Grant et al (2016), who demonstrated that following monocular enucleation at P0, layer V axons rearrange and grow abberantly in the dLGN (Grant et al, 2016). Subsequent study by Frangeul et al (2016) has also showed a cross-hierarchical effect in the dLGN after input deprivation, with layer V axons from V1 evoking synaptic terminals in dLGN neurons, an effect elicited normally in LP neurons only (Frangeul et al, 2016). Therefore, an aspect of cross-hierachical plasticity that I was intending to examine was the size and density of GFP-VGluT1 positive synapses formed in the enucleated conditions in the dLGN and compare them with the LP-formed synapses, expecting to detect similarity in their characteristics. However, the possible leaky expression of the Cre-independent virus used for the performance of the experiments, has compromised the specificity of the analysis I was aiming to perform, as GFP+ projections and synaptic boutons in dLGN and LP could have been derived from other cortical layers, most probably from layer VI. Consequently, I decided not to proceed with the comparison of the size and density of the GFP+ VGluT1+ boutons in dLGN and LP after visual deprivation as there was an increased risk of quantifying synaptic boutons of different cortical origin than layer V.

After performance of Cre-independent GFP viral injections in V1 and S1 of control and monocularly enucleated Rbp4-Cre::tdTom brains (Fig.3.1.3., A; 3 brains were used per condition), I have identified V1 and not S1 as the source of the rearranged GFP+ fibres found in the enucleated dLGN. Subsequently, I examined the expression pattern of these GFP+ fibres originating from V1 to the dLGN. In control conditions, these axons pass through the medial part of the dLGN, showing a wide expression in the centre of the structure colocalizing with the tdTom fibres (Fig.3.1.3., B-B2). In the enucleated brains, GFP+ axons demonstrated a rearrangement in the lower ventro-lateral part of the dLGN (Fig.3.1.3., C-C2), with a small number of axons passing through the dorsal part of the structure and colocalizing with the tdTom+ rewired fibres (white arrows in Fig.3.1.3., C-C2). Furthermore, I performed immunostaining against VGluT1 for quantification of the tdTom+ VGluT1+ synaptic boutons formed in the control and enucleated dorsomedial part of the dLGN of different brains (white boxes in Fig.3.1.3., B and C respectively) to specify the effect of enucleation in the structure. The quantification showed a significant difference in the formation of synaptic boutons per mm^2 of dLGN area, with the density of boutons to have been significantly increased in the dLGN of enucleated brains in comparison with the dLGN bouton density in control brains (Fig.3.1.3., D; $n=3$, at least 3 medial sections per brain, $p<0.0001$, Mann Whitney, two-tailed, unpaired Student’s t-test). This result indicated that following enucleation, layer V axons were not only passing through the dLGN, but sprouted forming synapses, An effect normally observed in the LP, which might indicate that the deprived dLGN acquired HO-like characteristics after input deprivation.

Following, I examined the expression pattern of the GFP+ axons reaching the LP after passing through dLGN. In the control conditions, the axons passed through the medial dLGN and reached LP, and more specifically LPLR, showing colocalization with the tdTom+ fibres (Fig 3.1.3., E-E2). A similar pattern was observed in the enucleated brains where no apparent difference was found in the ingrowth of GFP+ axons to the structure, with rearranged axons coming from the lower ventro-lateral dLGN eventually reaching the LPLR and colocalizing with the tdTom+ fibres (Fig. 3.1.3., F-F2).

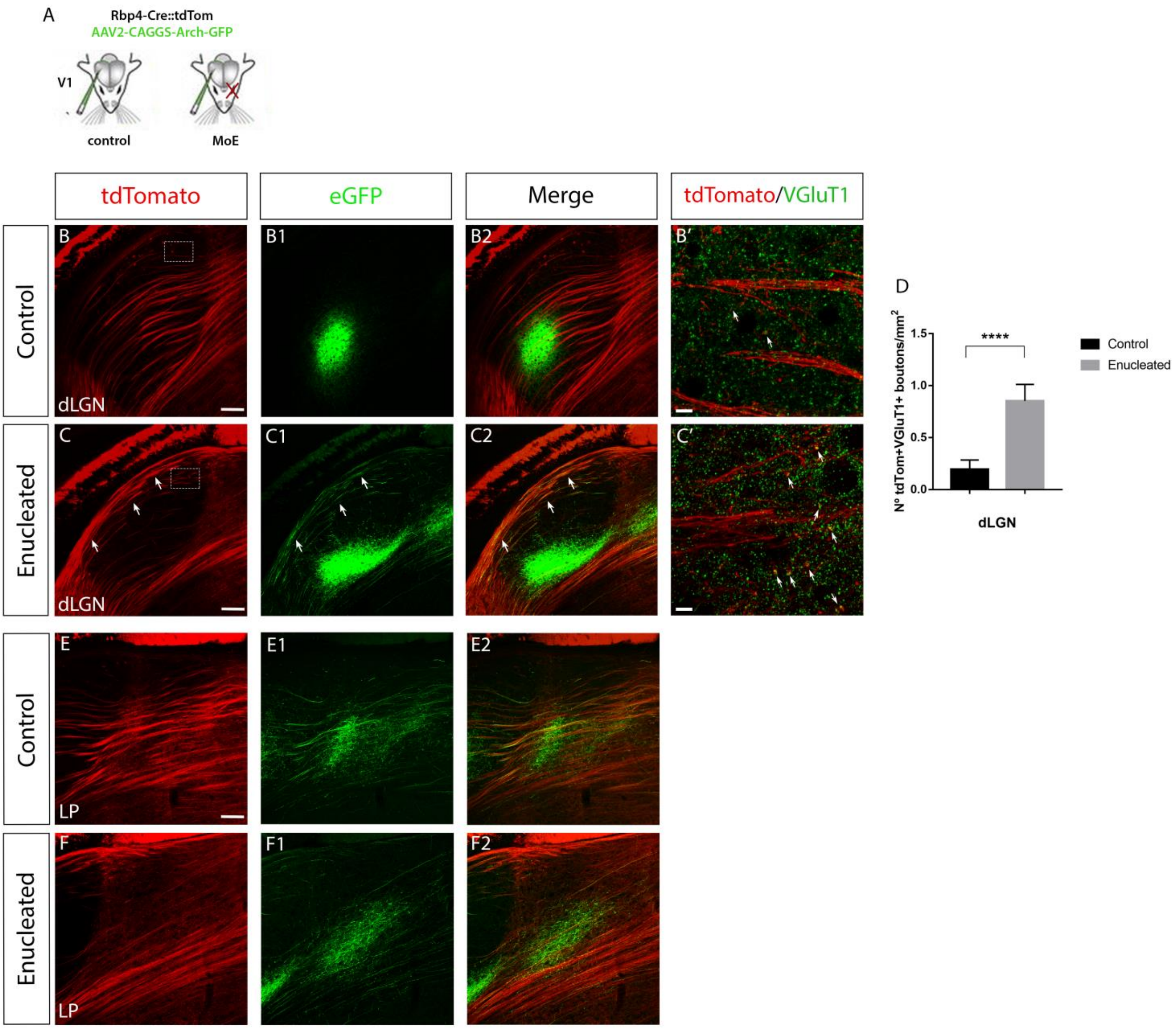

Figure 3.1.3. Pattern of Layer V AAV-GFP positive corticothalamic projection ingrowth into the control and enucleated dLGN and LP. (A) Schema representing the experimental design of the AAV GFP Cre-independent injections in primary visual cortex (V1) in control and monocularly enucleated (MoE) Rbp4-Cre::tdTomato adult mice. (B-B2) In control dLGN, GFP+ axons project through the centre of the structure, whereas in the enucleated dLGN (C-C2), GFP+ axons traverse the lower lateral ventral part of the structure with few axons detected to sprout through the dorsal part of dLGN and colocalize with the rearranged tdTomato fibres (white arrows). (B’, C’) High magnification images of the demarcated area in images B and C respectively, showing very few boutons formed in the control dLGN in comparison with the enucleated dLGN, where there is a significant increase in the synapse formation, as shown in graph (D). (E-E2) In control conditions, Layer V GFP+ fibres that grow through dLGN, reach the LP and specifically LPLR. (F-F2) In the enucleated hemisphere, GFP+ axons coming from the lower ventro-lateral dLGN, reach LPLR showing similar expression pattern with the control conditions. Results for quantifications based on n=3 animals, at least 3 medial sections per animal. Values shown are mean and standard error. ****= significant at $p<0.0001$. Abbreviations: dLGN, dorsal lateral geniculate nucleus; LP, lateral posterior nucleus; GFP, green fluorescent protein; VGluT1, vesicular glutamate transporter 1. Scale bars: 100 µm (B-B2, C-C2, E-F2), 10 µm (B’, C’).

3.2. The effect of monocular enucleation on gene expression in dLGN

Previous unpublished research from our laboratory performed by Dr Eleanor Grant focused on the effect of peripheral input deprivation in the transcriptional profile of dLGN in early developmental stages, demonstrating a delay in the maturation of the dLGN transcriptome after visual deprivation. Firstly, mice were monocularly enucleated at P0 and subsequently control and enucleated dLGN were collected at P6, when the effect of cross-hierarchical rewiring was first shown (Grant et al, 2016). Following, microarray gene expression analysis was performed, revealing a plethora of genes that were differentially expressed in the dLGN after input deprivation. These results were also confirmed by qPCR experiments, identifying 22 genes with altered expression in the dLGN after MoE.

For my experiments, 5 of these 22 genes were selected for validation of their expression in control and enucleated dLGN by *in situ* hybridization. These genes were *Otx2*, *Kcnk9*, *EphrinA5*, *Calbindin2* and *Cerebellin2* and were selected based on their different molecular function.

Although the microarray and qPCR analysis were performed at P6, I decided to use tissue collected from control and enucleated mice at P8. This was due to a problem in harvesting good-quality cryosections at P6, resulting in serious tissue damage throughout the performance of the *in situ* experiments. Therefore, P8 was chosen as a good age for examining the expression patterns of the selected genes as it is the age where synaptic formation is firstly demonstrated in dLGN after MoE (Grant et al, 2016). What is more, gene expression on tissue from P6 brains that were not destroyed during the experiments was compared with that on P8 brains, showing high similarity between them (data not shown).

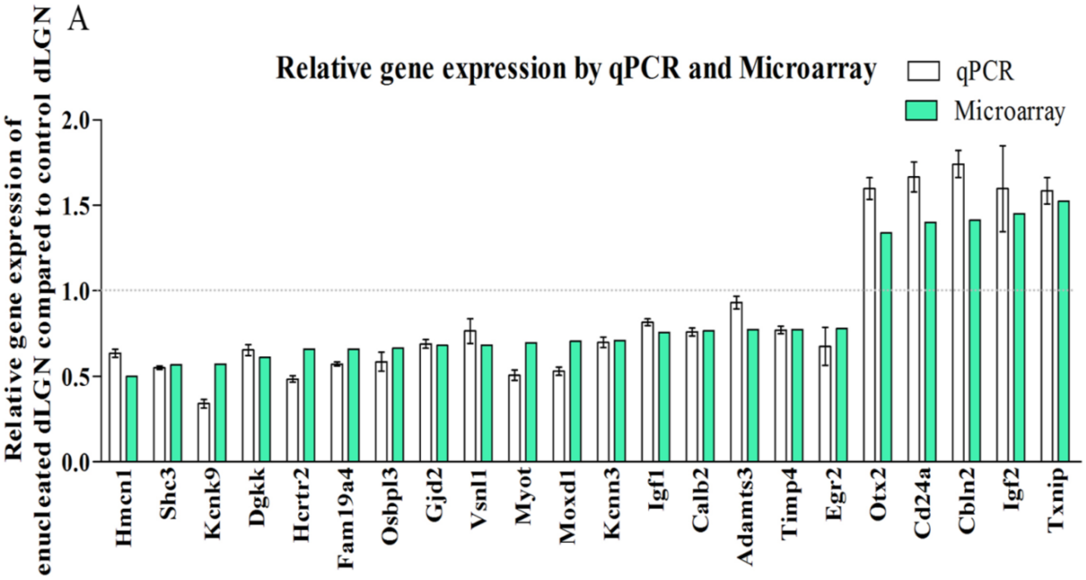

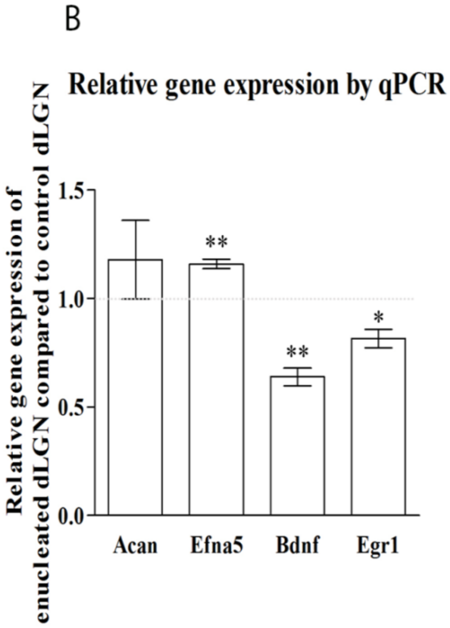

Figure 3.2.1. Gene expression changes in dLGN at P6 after P0 MoE show mostly down-regulated genes. (A) Graph showing relative expression levels of genes in enucleated compared to control dLGN as assessed by qPCR and microarray. Relative expression of all genes, as assessed by qPCR, was in the same direction as relative expression assessed by the microarray. (B) Graph showing relative expression by qPCR in enucleated dLGN compared to control dLGN of genes identified by biological interest. Aggrecan was not significantly differently expressed. EprhinA5 was significantly increased in the enucleated dLGN compared to control dLGN. BDNF was significantly decreased in enucleated dLGN compared to control dLGN. Early growth response 1 was significantly decreased in enucleated dLGN compared to control dLGN. Values shown are mean and standard error. *= significant at p=0.05, **= significant at p=0.005 (E Grant et al., unpublished data).

Otx2 is a transcription factor, which is considered essential for the regulation of interneuron development, migration and plasticity in the visual system. It is expressed specifically by dLGN GABAergic interneurons and not dLGN thalamocortical neurons. It has also been demonstrated to be expressed in a subpopulation of interneurons in the ventral LGN (vLGN), indicating common origins with the interneurons expressing Otx2 in dLGN (Golding et al, 2013; Sugiyama et al, 2008). Otx2 was found to be upregulated in the dLGN in our microarray after monocular enucleation. This change was validated by the *in situ* experiments performed, where the pattern of expression showed an upregulation in the enucleated dLGN in comparison with the control (Fig.3.2.2. B and A respectively). In the control side, a few cells were distinctly labelled in the structure (Fig.3.2.2. A, C), whereas in the deprived side the number of labelled cells was increased, with cells occupying the majority of the dLGN area (Fig.3.2.2. B, D). What is more, from quantifications of fluorescent *in situ* sections, it was found that this upregulation observed in the expression of Otx2 in the enucleated dLGN was significant (n=3; p=0.0117, Wilcoxon, two-tailed, paired Student’s t-test).

Cerebellin 2 precursor protein (Cbln2) is a synaptic organizer localized in Purkinje cells having a role in synaptogenesis. In normal conditions, Cbln2 is showing a downregulation in dLGN over development. (Singh et al, 2012). In our microarray, it was detected to be upregulated in the enucleated dLGN compared to the control ((Fig.3.2.2. G and F respectively; n=3; p=0.25, Wilcoxon, two-tailed, paired Student’s t-test).

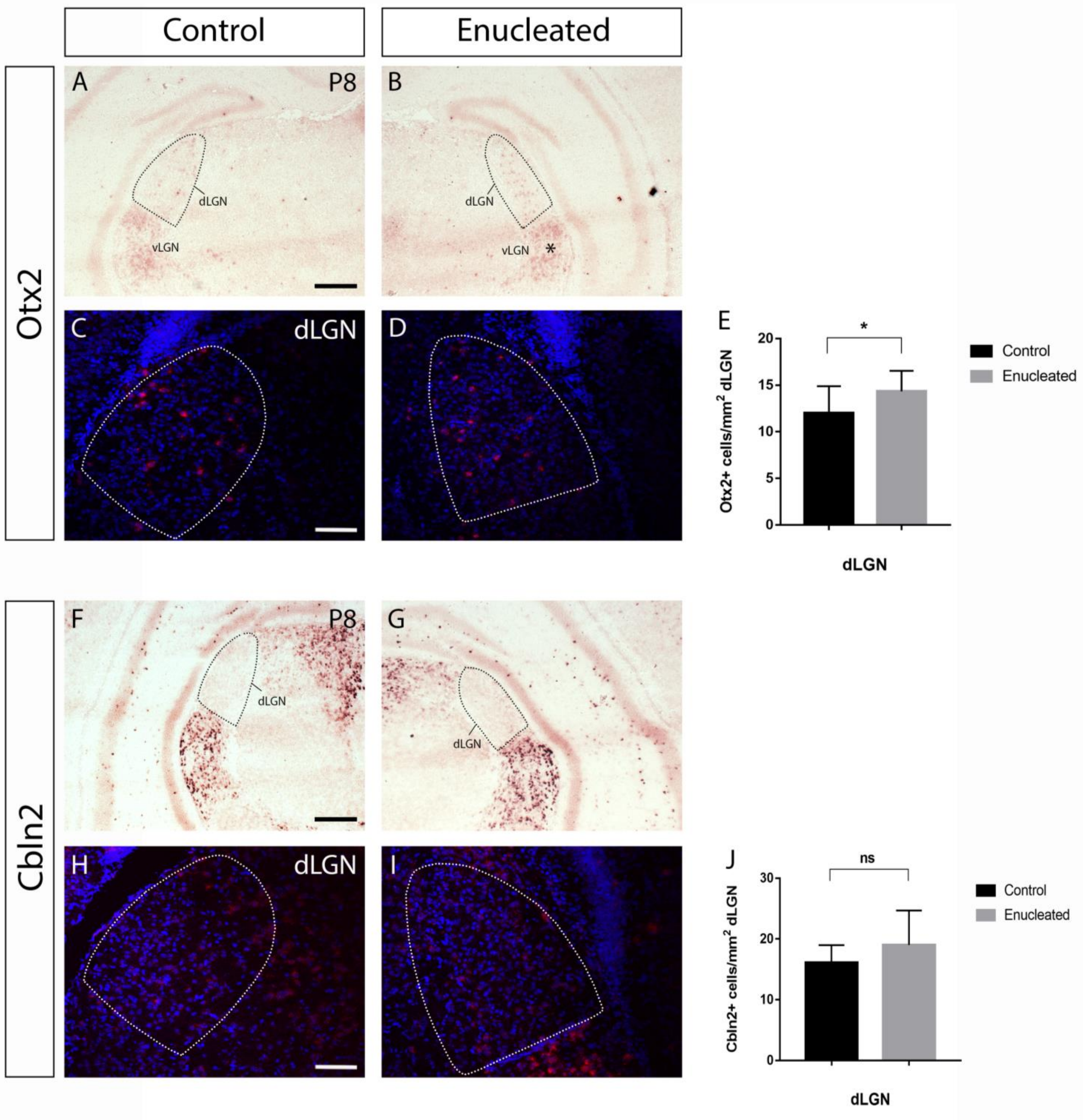

Figure 3.2.2. *In situ* hybridization of Otx2 and Cbln2 expression in coronal sections of control and enucleated Rbp4-Cre brains at P8. Otx2 expression was found to be increased (E) in enucleated dLGN and vLGN (asterisk) (B, D) compared to the control (A, C). Cbln2 expression was upregulated (J) in enucleated dLGN (G, I) in comparison to the control side (F, H). Abbreviations: Otx2, orthodenticle homologue 2; Cbln2, cerebellin 2 precursor protein; dLGN, dorsal lateral geniculate nucleus; vLGN, ventral lateral geniculate nucleus. Scale bars: 200μm.

Calbindin2 (Calb2), also known as calretinin, is a calcium-sensitive protein expressed in dLGN interneurons, demonstrating an upregulation in the structure over development. This population of Calb2+ interneurons is different from the population expressing Otx2 in the dLGN (Beurdeley et al, 2012). Calb2 was found to be downregulated in the deprived dLGN in our microarray. Its expression pattern from the *in situ* experiments indicated a decrease in the Calb2 positive cells in the enucleated dLGN (Fig.3.2.3. B, D); however, after quantification of the density of Calb2+ cells in the dLGN, this decrease was not found to be significant (n=3; p=0.0625, Wilcoxon, two-tailed, paired Student's t-test).

Potassium channel K9 (Kcnk9) is a potassium-selected leak channel, exhibiting an important role in the regulation of cell division and migration as well as in the establishment of resting membrane potential and thus neuronal excitability (Goldstein et al, 2001). It is expressed in many types of neurons in the developing mouse brain in the first two postnatal weeks, showing high levels of expression in the cerebral cortex and the cerebellum (Aller and Wisden, 2008). In our results, the expression of Kcnk9 was found to label distinctly cells in the control dLGN and shown to be downregulated in the deprived dLGN (Fig.3.2.3. F and G respectively), but not significantly (n=3; p=0.125, Wilcoxon, two-tailed, paired Student's t-test).

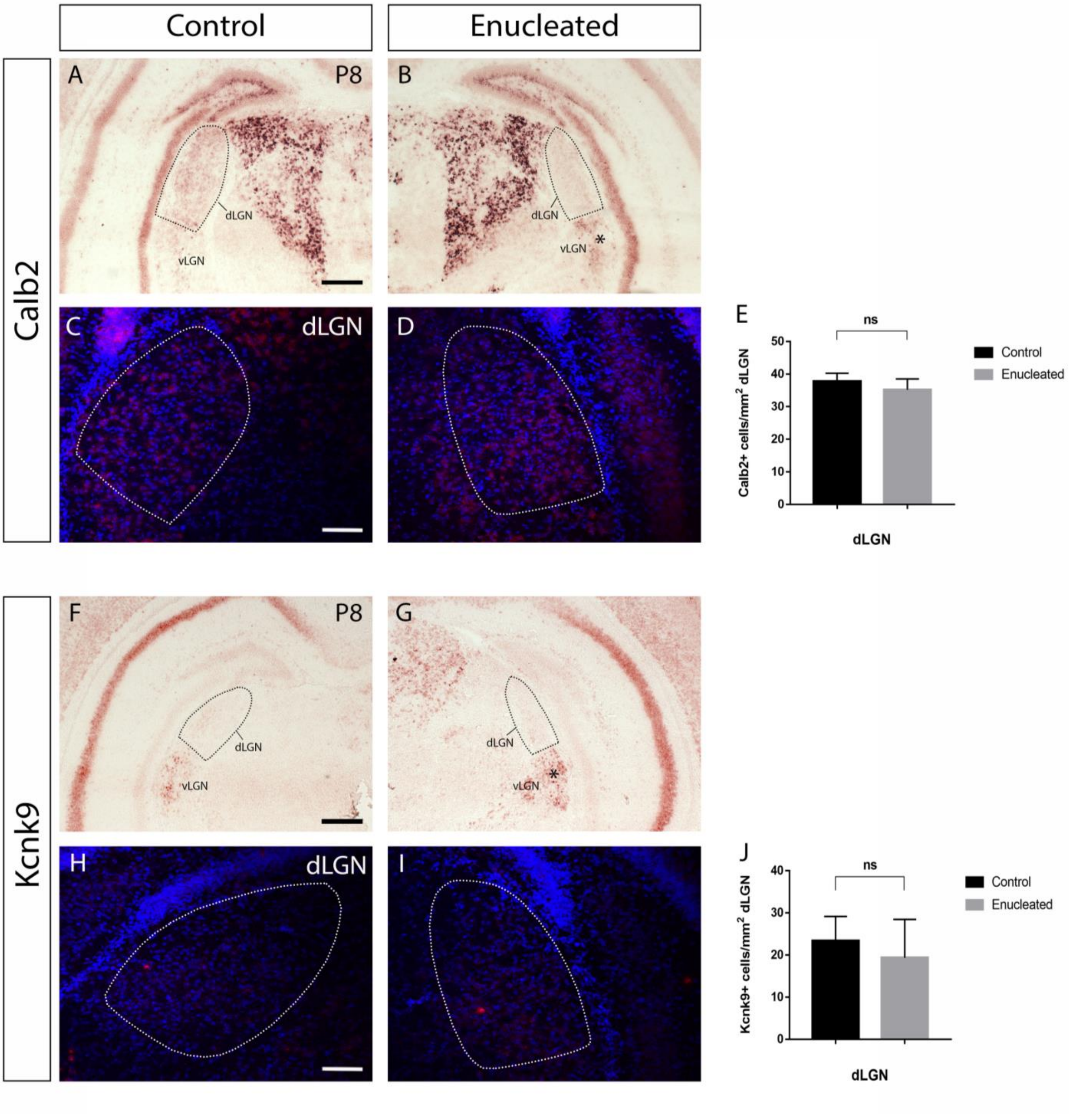

Figure 3.2.3. ***In situ*** **hybridization of Calb2 and Kcnk9 expression in coronal sections of control and enucleated Rbp4-Cre brains at P8.** Calb2 expression was found to be decreased (E) in enucleated dLGN (B, D) compared to the control side (A, C). Kchk9 expression was downregulated in enucleated dLGN (G, I) compared to the control hemisphere (F, H); however, expression in vLGN was shown to be increased in the deprived hemisphere for both genes (asterisks in B and G respectively) in comparison with the control hemisphere. Abbreviations: Calb2, calbindin 2; Kcnk9, potassium channel, subfamily K, member 9; dLGN, dorsal lateral geniculate nucleus; vLGN, ventral lateral geniculate nucleus. Scale bars: 200μm.

EphrinA5 is a cell surface-bound ligand for the Eph receptor family. In the thalamocortical system, EphrinA5 has been characterized for its repellent activity for somatosensory thalamocortical axons that express Eph receptors. Additionally, it was shown to play a role in the regulation and specificity of the topography of thalamocortical projections within specific cortical areas, including retinotopy in the visual system (Vanderhaegen et al, 2000; Dufour et al, 2003). In the molecular analysis performed previously in our laboratory, EphrinA5 was selected out of biological interest for validation of its expression in dLGN by qPCR following monocular enucleation. The results of the qPCR revealed a significant increase in the expression of this gene in the deprived dLGN at P6. This result contradicts with previous study by Dye et al (2012), where it was shown by *in situ* hybridization that the area of expression of EphrinA5 was decreased in dLGN after enucleation (Dye et al, 2012). My *in situ* results could not validate the qPCR results as the expression of EphrinA5 showed a downregulation in the deprived dLGN in comparison to the control (Fig.3.2.4. B and A respectively), an expression pattern similar to the one reported in the study from Dye et al (2012); however, this reduced expression was not significant (n=3; p=0.375, Wilcoxon, two-tailed, paired Student's t-test). Moreover, an interesting expression pattern was found in the expression levels in dLGN and LP. More specifically, EphrinA5 was strongly expressed in dLGN in the control hemisphere in comparison with the LP labelling. However, in the enucleated side, this differential expression between the two structures was no longer evident.

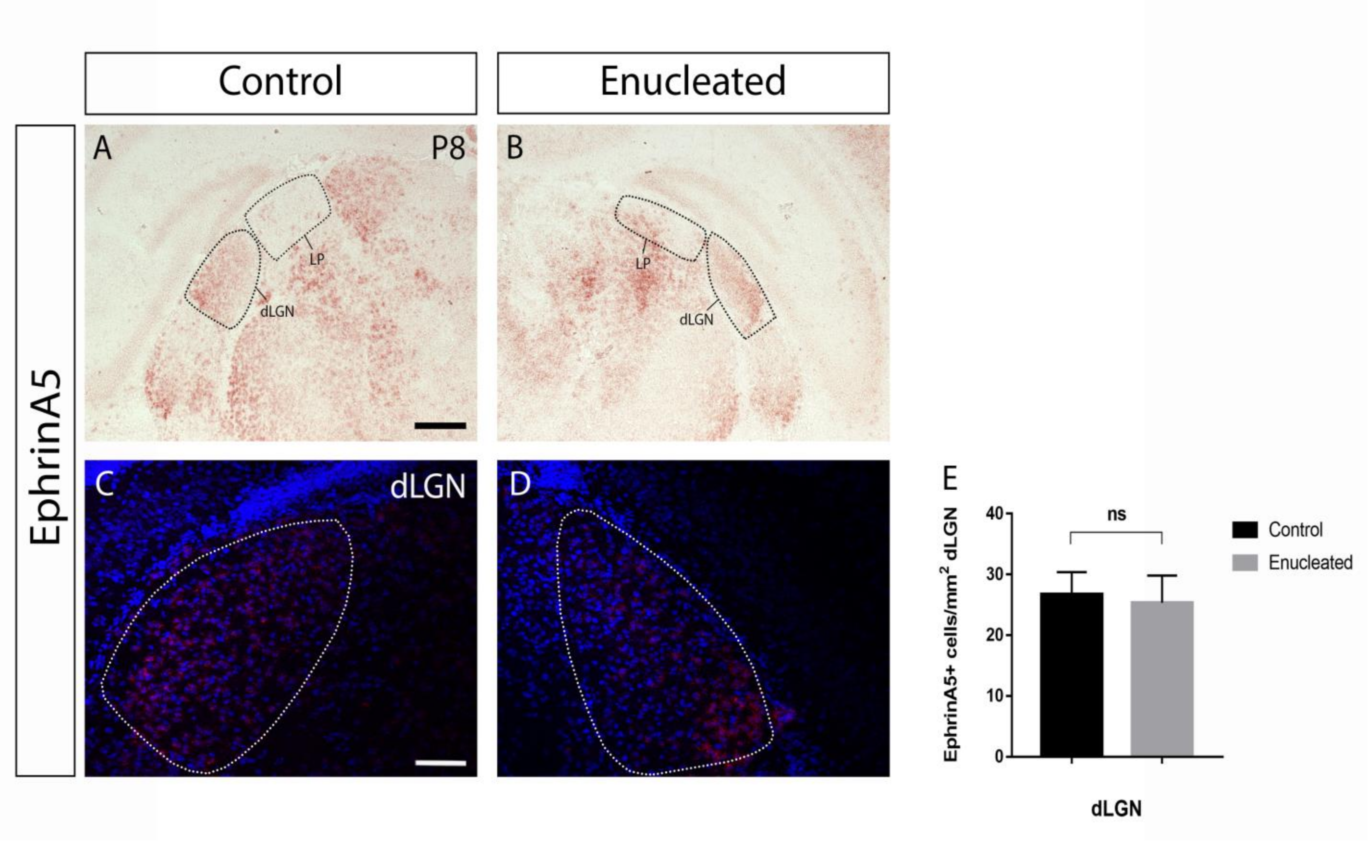

Figure 3.2.4. *In situ* hybridization of EphrinA5 expression in coronal sections of control and enucleated Rbp4-Cre brains at P8. EphrinA5 expression was found to be downregulated (E) in the enucleated dLGN (B, D) in comparison to the control (A, C). This result contradicted with the qPCR results previously obtained in my laboratory, which indicated an increase of EphrinA5 expression following enucleation. In addition, an increase in the EphrinA5 expression was observed in the LP of the enucleated hemisphere (B) in comparison to the control side (A). Note the differential expression levels in lateral posterior (LP) and dorsal geniculate nucleus (dLGN) in control with dLGN having the stronger label (A). These differences are no longer evident after enucleation in the dLGN of reduced volume, with dLGN and LP showing similar expression levels (B). Abbreviations: dLGN, dorsal lateral geniculate nucleus; LP, lateral posterior nucleus. Scale bars: 200µm.

4. Discussion

The mechanisms involved in the regulation of the development and plasticity of corticothalamic projections has been largely neglected in the past with most studies focusing on the afferents from the periphery to the subcortical structures and from the thalamus to the cortex. In this study, my aim was to identify the origin of corticofugal projections coming from crtical layer V to the thalamus after visual deprivation by MoE. Furthermore, focusing on previously reported cross-hierarchical plasticity in dLGN (Grant et al, 2016) following input ablation, I studied the effects of peripheral input in the specification of dLGN functional and transcriptional profile.

4.1. Do corticothalamic axons originate only from V1 after peripheral manipulation?

My results from the viral tracing study demonstrated that, after peripheral input deprivation by MoE, corticothalamic axons originate from V1 and not from S1. Projections coming from V1 were reaching the latero-ventral part of dLGN, eventually sprouting into LP. On the other hand, no alterations in the S1 projections to thalamus were observed following MoE with S1 axons completely bypassing dLGN. S1 projections were only found to innervate and sprout in the somatosensory thalamic nuclei, the first-order VPM and the higher-order Po. However, the expression of the virus was shown to be higher in VPM and not Po as normally expected from layer V projections that reach and sprout in higher-order nuclei. This might be due to contamination of layer VI with the virus in the injections site as projections from this layer reach both first-order and higher-order thalamic nuclei. Nevertheless, origin results were not affected as projections from S1 were not found to rearrange to innervate dLGN, which demonstrated that S1 was not the origin of layer V projections after retinal input deprivation.

Although S1 did not appear to be the origin of layer V projections to dLGN following MoE, further research should be performed on A1 involvement in layer V development in dLGN. Many studies by using different manipulations in the visual or auditory system, have previously revealed the existence of cross-modal plasticity between them.

In neonatal ferrets, it has been shown that retinal axons are rewired in order to innervate the medial geniculate nucleus (MGN) in addition to the dLGN thus inducing cross-modal plasticity with visual inputs eventually driving the auditory cortex. This was achieved by unilateral or bilateral lesioning of the inferior colliculus and cochlea that normally provides input to the auditory thalamus. As a result of this plastic effect, the rewired auditory cortex was responsive to visual stimuli, the rewired cortical neurons acquired similar orientation and direction selectivity to the ones in the visual cortex, and finally, the long-range connections formed resembled the ones found in the primary visual cortex (Sur et al, 1988; Roe et al, 1992; Angelucci et al., 1997; Angelucci et al., 1998). This example of cross-modal plasticity is characteristic for exhibiting the role of visual activity in shaping and remodelling intracortical circuitry.

Cross-modal rewiring was also found previously in humans. In congenitally blind individuals, the visual cortex was activated by somatosensory and auditory stimuli (Cohen et al, 1997), while in congenitally deaf individuals, activation of the auditory cortex was observed in response to visual stimuli (Bavelier and Neville, 2002).

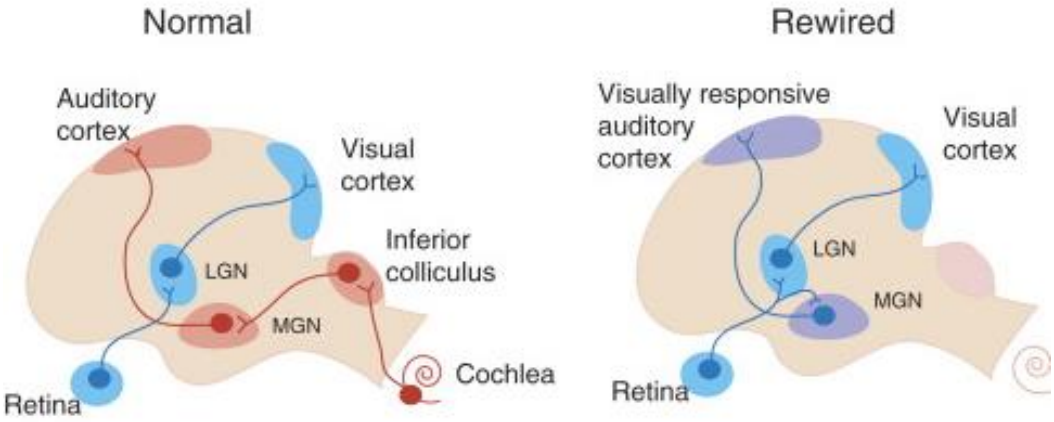

Figure 4.1. Cross-modal connectivity and plasticity between visual and auditory systems following input deprivation. In the visual pathway, retinal afferents innervate the dorsal lateral geniculate nucleus (dLGN) and the superior colliculus (SC), with dLGN projecting to the primary visual cortex (V1). In the auditory pathway, afferents from the cochlear nucleus reach the inferior colliculus (IC), continuing to the medial geniculate nucleus (MGN) and the amygdala, eventually arriving to the primary auditory cortex (A1). Input ablation of the IC in neonatal animals induces retinal afferents to innervate the MGN and reorganize the auditory cortex in order to process visual input. Adapted by Horng and Sur, 2006.

Furthermore, in the dorsal area of dLGN, where the thick bundle of tdTom+ fibres was identified after MoE as a sign of axon rearrangement inside dLGN, very few GFP+ projections were found to cross through this specific area and overlay with the tdTom+ fibres. Thus, it is possible that this bundle of tdTom+ fibres in the dorsal dLGN might not derive exclusively from V1. Additionally, we have shown that these fibres do not originate from S1. Thus, it could be suggested that either there is a cross-modal plastic effect with these fibres originating from A1, or they might derive from another secondary area of the visual cortex, such as V2, indicating that the plasticity might be occurring inside the visual cortex.

The latter can be supported from previous research from Pouchelon et al (2014), where it was demonstrated that in the somatosensory cortex following input deprivation by infraorbital nerve sectioning, the S1 circuits formed acquire S2-like properties, thus first-order thalamic input is essential for the acquisition of associative cortical identity (Pouchelon et al, 2014). What is more, it has been shown that primary cortical areas such as V1 and S1, acquire transcriptional characteristics of their associative secondary cortical areas (V2 and S2, respectively) in the absence of thalamocortical input, indicating the importance of exteroceptive thalamic input in the differentiation of cortical areas of the same sensory modality (Pouchelon et al, 2014; Chou et al, 2013; Vue et al, 2013).

Therefore, projections from A1 or other sources, such as secondary cortical areas, should also be further investigated in order to define the exact origin of projections after visual deprivation in different parts of dLGN and whether the plastic effects observed following MoE is regulated by multiple cortical areas.

4.2. Does retinal input affects synaptic formation in dLGN?

Corticothalamic axons start to innervate the dLGN at P3 (Brooks et al, 2013; Seabrook et al, 2013; Grant et al, 2016). As for retinogeniculate axons, although they are present in the thalamus from E15.5 (Deck et al, 2013; Moreno-Juan et al, 2017), they do not innervate and form functional synapses in the dLGN until P12 (Brooks et al, 2013; Seabrook et al, 2013; Grant et al, 2016). The majority of synapses present in dLGN arise from layer VI corticothalamic neurons from V1, brainstem nuclei and TRN inputs (Briggs and Usrey, 2008; Sherman and Guillery, 2002). Interestingly, retinal inputs comprise only 10% of the total amount of synapses found in the dLGN (Sherman and Guillery, 2002; Bickford et al, 2010). However, the importance of retinogeniculate axons in shaping the topography of corticothalamic axons in the dLGN has been recently shown. More specifically, when mice were monocularly enucleated at birth, layer V corticothalamic axons prematurely enter the dLGN (Grant et al, 2016).

Additionally, Seabrook et al (2013) have showed that upon retinal inout abolishment either by binocular enucleation at birth or genetically, layer VI enters dLGN prematurely (Seabrook et al, 2013). What is more, visual deprivation during thalamic critical period has led to a redistribution of boutons in the broad axon arbor rather than large scale sprouting and retraction of axonal segments (Hong et al, 2014), showing the role of peripheral activity in synaptic bouton physiology.

My research showed that after MoE, there is a significant increase in the formation of layer V boutons in the deprived dLGN in comparison with the control dLGN in the same brain. In the control dLGN, as expected, minimum number of synapses was found, as in normal conditions, layer V axons just cross through dLGN without sprouting. The significant increase in layer V synaptic formation after MoE might be an outcome of cross-hierarchical plasticity between the first-order dLGN and the higher-order LP and could indicate the essential role of peripheral input in thalamic nuclei classification. Recent study by Pouchelon et al (2014) has shown a cross-hierarchical plastic change in the somatosensory system, where genetic ablation of the first-order VPM has induced input rewiring from the higher-order Po into layer IV of S1 (Pouchelon et al, 2014).

The original aim of my research after identifying the origin of the layer V corticothalamic projections would have been to measure the size and density of the GFP+ VGluT1+ synaptic boutons formed in the enucleated dLGN and compare these measurements with the GFP+ VGluT1+ boutons formed in LP. I hypothesized that the formed synapses in the “deprived” dLGN would have been more similar in size to the synapses formed in LP, indicating that they would have gained a driver-like synapse morphology found in the HO thalamic nuclei (Sherman and Guillery, 2002). This hypothesis was based on previous research from Frangeul et al (2016), in which the authors have demonstrated that, in the absence of peripheral input by binocular enucleation at P0, optogenetic stimulation of layer V axons in V1 elicits postsynaptic terminals in the input-ablated dLGN neurons. This revealed that loss of peripheral input results in the acquisition of HO cortical input by FO neurons, matching with the anatomical data showing cross-hierarchical rewiring in dLGN after MoE at P0 (Grant et al, 2016). Therefore, future research in which I am going to be able to evaluate the synaptic boutons arising from layer V rearranged axons in the enucleated dLGN would be essential for evaluating the effect of retinal input in the acquisition of the synaptic characteristics in the different thalamic nuclei.

4.3. Do molecular mechanisms regulate the development of corticothalamic axons into dLGN?

In the last decades, the research in developmental neurobiology has been focused in identifying the implication of extrinsic activity in the determination of neuronal identity and function. A persistent question around this subject is the interaction between peripheral input and intrinsic genetic programs and to which extent it instructs the establishment of neuronal characteristics, functional connectivity and differentiation of regions in the cortical and subcortical areas.

In order to evaluate the role of peripheral input in the regulation of activity-dependent molecular mechanisms in the visual thalamic nuclei, a microarray gene expression analysis was performed in the dLGN following enucleation (Grant et al, 2016, unpublished). Immediate early genes including BDNF, Egr1 and Egr2, genes involved in neuronal activity, such as Kcnn3 and Kcnk9, and the kinase pathway molecules Dgkk and Shc3, was detected to be differentially expressed after loss of peripheral input. The majority of these genes are normally regulated during the first postnatal weeks of development, which might indicate a delay in the maturation of the dLGN transcriptome due to absence of retinal activity.

Recent study in mice has shown that when retinal input was rewired to MGN, there was a change in the normal MGN transcriptome, with genes that are normally expressed in the dLGN to start express in the MGN, indicating a modality-specific input regulation of gene expression (Horng et al, 2009). More specifically, 10 genes that are dLGN-specific were found to be upregulated in the rewired MGN at P5, including the zinc-finger transcription factor, Zic4 (Horng et al, 2009), which is strongly enriched in dLGN and has an important role in visual pathway development (Pak et al, 2004).

Transcriptomic changes to S1-S2 L4 neurons following IONS have also been revealed by Pouchelon et al (2014). More specifically, a microarray gene expression analysis performed at P10 showed that a VB to Po switch induced changes in the defined S1L4- and S2L4-type transcripts, with S1L4 neurons acquiring a more similar molecular identity to S2L4 neurons after input deprivation. Therefore, distinct TC inputs mediate the functional molecular features of postsynaptic L4 cortical neurons in a modality-specific manner with only a specific subset of S1L4- and S2L4-type genes was affected from VB and Po input changes (Pouchelon et al, 2014). What is more, Moreno-Juan and colleagues (2017) have demonstrated that after embryonic binocular enucleation in mice at E14.5 before retinal axons reach the thalamus, not only has led to an increase in the size of the cortical barrel field in S1 at P4, but also changes in the transcriptional profile of the VPM, the corresponding somatosensory thalamic nucleus, at P0 and P4, with the RAR-related orphan receptor B (Rorβ), which has been previously shown to influence somatosensory cortical development (Jabaudon et al, 2012), to be found significantly increased after visual deprivation (Moreno-Juan et al, 2017).

In recent genetic work, it has been shown that interestingly, following binocular enucleation at birth, as well as IONS to sensory ablate VPM, FO nuclei acquired a transcriptional profile that was more similar to that of HO nuclei, supporting the hypothesis that HO identity is a default state (Frangeul et al, 2016). According to this theory, synapses originally hold HO characteristics in both first-order and higher-order thalamic nuclei and due to peripheral input, they eventually adopt their FO characteristics; thus FO identity is subsequently acquired in an input-dependent manner (Bishop, 1959; Butler, 2008; Frangeul et al, 2016). From an evolutionary point of view, all the aforementioned findings of cross-hierarchical plasticity and rewiring support the idea that neurons with HO-like identity might be ancestors of neurons located in FO thalamic nuclei and primary cortical areas, with the latter emerging from a pool of higher-order neurons based on the connectivity, electrophysiological and metabolic characteristics (Frangeul et al, 2016).

Genetic ablation of retinal input with the *math5*$^{-/-}$ mouse model as well as induced input deprivation by binocular enucleation at birth have shown acceleration of the timing of innervation of Layer VI axons to the dLGN (Seabrook et al, 2013). What is more, the same group revealed the role of aggrecan (chondroitin sulfate proteoglycan 1), an extracellular matrix protein that belongs to the perineuronal net family, in the timing of entrance of Layer VI axons in the dLGN, demonstrating that after loss of retinal input, aggrecan is driving Layer VI and VIb axons to prematurely enter to the dLGN (Brooks et al, 2013). These results have proposed that retinal inputs might initially prevent the expression of endogenous aggrecanases by dLGN relay neurons.

In my study, I investigated by *in situ* hybridization the expression of 5 genes, *Otx2*, *Kcnk9*, *EphrinA5*, *Calb2* and *Cbln2*, aiming to validate the microarray and qPCR data obtained by my laboratory. Although my qualitative results from the *in situ* experiments showed an altered expression pattern in the control and enucleated dLGN for all the genes, quantification results were only found to be significant for Otx2. This might be due to the manner of quantification used as *in situ* hybridization is not an absolute method for quantifying gene expression. However, it was useful for a first identification of the mRNA expression of each gene, but for performance of immunostaining would be necessary for a complete analysis of cell density in the dLGN. Therefore, in this chapter, I am going to focus on two genes based on my results and their biological significance; a) Otx2, which gave a clear expression pattern and significant upregulation in the deprived dLGN, and b) EphrinA5, which although it was not significantly altered after quantification of its cell density in the dLGN, it showed an interesting expression pattern change in the visual thalamic nuclei following enucleation.

Role of Otx2 in critical period plasticity in the dLGN?

My results showed a significant increase in the expression of Otx2 in the dLGN. This result validated the microarray and qPCR analysis previously performed in my laboratory, also revealing an increase in the vLGN expression of Otx2+ cells. This might indicate a delay of interneurons to enter the dLGN possibly due to the loss of peripheral input, thus revealing the effect of peripheral input in the timing of interneuron migration to dLGN.

Specific transfer of Otx2 and BDNF to GABAergic inhibitory parvalbumin interneurons, which receive the most potent direct thalamocortical input, is essential and sufficient for the onset of the critical period of plasticity in the developing murine visual cortex by endogenously coordinating parvalbumin cell maturation (Sugiyama et al, 2008). The accumulation of Otx2 in these cells is a non-cell autonomous process, with Otx2 to be transferred from other areas, such as the retina and dLGN, to V1 and its capture to be dependent upon visual input as it has been reported to be reduced in the visual cortex upon dark rearing (Sugiyama et al, 2008). At critical period onset, sensory input induces the formation of perineuronal nets, a specialized glycosaminoglycan-rich extracellular matrix (Pizzorusso et al, 2002), on the surface of parvalbumin interneurons. Perineuronal nets regulate the persistent internalization of Otx2 endogenously by parvalbumin cells, thus acting as molecular brakes to maintain critical period closure (Sugiyama et al, 2008; Beurdeley et al, 2012). Therefore, interaction of Otx2 and perineuronal nets is necessary for the modulation of critical period plasticity in the visual cortex. However, the effect of the interaction of Otx2 with perineuronal nets and parvalbumin interneurons in the dLGN is still unknown. Brooks et al (2013) have reported that the presence of perineuronal nets and particularly, aggrecan in the dLGN plays a role in the regulation of the timing of layer VI axon innervation to the structure. Moreover, a recent study from Golding and colleagues (2014) has shown affected migration and incorporation Otx2+ interneurons into the dLGN, demonstrating a reorganization of this population at the dorsal part of dLGN at P20 after bilateral enucleation at birth. (Golding et al, 2014). Therefore, my results in combination with these studies might reveal a potential role of Otx2 in interaction with perineuronal nets in the regulation of critical period plasticity in the dLGN, which could be experience-dependent.

Role of EphrinA5 in guidance and rewiring of corticothalamic projections?

EphA-EphrinA signalling has been shown to be involved in the establishment of cortical areas and the guidance of thalamocortical projections in the visual system (Ellsworth et al, 2005). Experiments in double knockout EphrinA2/A5 mice, in which input ablation was induced, showed that rewiring was increased in the lack of these Ephrin ligands for which retinal axons have receptors

(Lyckman et al, 2001). However, just the absence of these ligands was not sufficient to induce rewiring, indicating the role of molecular cues in the guidance of sensory afferents to their respective thalamic areas. Therefore, except of the role of activity, the necessity of intrinsic molecular cues in the remodelling of corticothalamic and thalamocortical connections has to be considered. Additionally, alteration of the interaction of ephrinA gradients in the cortex by the use of ephrinA2/A3/A5 knockout mice resulted in changes in the size and location of visual cortices (Cang et al, 2005), indicating that changes in the expression of this molecule might induce alterations in circuit formation.

What is more, Dye et al (2012) have demonstrated by *in situ* hybridization a downregulation in the expression of EphrinA5 in the dLGN after binocular enucleation at birth (Dye at al, 2012). My results confirmed this expression pattern showing a downregulation of the expression of EphrinA5 in the dlGN after visual deprivation, which unfortunately contradicts our qPCR results. However, the similarity in the expression of EphrinA5 in dLGN and LP following monocular enucleation observed in the *in situ* hybridization experiments could possibly indicate the role of retinal input in defining the transcriptional identity of the first-order and higher-order thalamic nuclei. This hypothesis could be also supported by the transcriptional analysis presented by Frangeul et al (2016), where the genetic profile of first-order nuclei was similar to the one in higher-order nuclei after input deprivation, suggesting that the determination of molecular identity of the different orders of thalamic nuclei is activity-dependent.

Future experiments investigating the functional relevance of the genes that are differentially expressed in the dLGN after monocular enucleation at birth are necessary for determining the mechanism and level of implication in the plasticity of corticothalamic axons that reach the dLGN. Overexpression of these genes in the enucleated dLGN by *in utero* electroporation in order to observe a blockage of the L5 ectopic sprouting, or depletion of these genes by shRNA in the control dLGN may induce L5 ectopic sprouting in the absence of retinal input alterations.

4.4. Concluding remarks

Despite a wide variety of studies performed the last decades trying to explore and understand the brain changes occurring upon sensory input deprivation, the identity of the brain areas that are altered as well as the exact mechanisms regulating cross-modal plasticity and the neural basis of behavioural compensation remain largely unknown. Further understanding of how the brain is rewired upon sensory loss is essential for unravelling the mechanisms underlying plasticity in the sensory deprived brain, thus gaining better insights into the translational investigation and possible therapeutic targets for individuals with a form of sensory deprivation. In this thesis, my results highlight the importance of peripheral input in the development and plasticity of the corticothalamic connections and the regulation of the transcriptional profile of thalamic nuclei. I showed that cross-hierarchical rewiring upon visual deprivation at birth is preserved until adulthood and that corticothalamic axons reaching the dLGN originate from V1 and not S1. Additionally, I have verified the molecular changes reported previously in the dLGN upon visual deprivation. These results allow us to hypothesise that early peripheral input to the thalamus contributes to the transcriptional and circuit hierarchy identity of thalamic nuclei. They also provide novel cues in the understanding of the compensatory mechanisms that the brain uses to adapt to changes and the increased capabilities in blind humans.

5. References

Aller, M. and Wisden, W. (2008). Changes in expression of some two-pore domain potassium channel genes (KCNK) in selected brain regions of developing mice. *Neuroscience*, 151(4), pp.1154-1172.

Altman, J. and Bayer, S. (1988). Development of the rat thalamus: I. Mosaic organization of the thalamic neuroepithelium. *The Journal of Comparative Neurology*, 275(3), pp.346-377.

Altman, J. and Bayer, S. (1988). Development of the rat thalamus: II. Time and site of origin and settling pattern of neurons derived from the anterior lobule of the thalamic neuroepithelium. *The Journal of Comparative Neurology*, 275(3), pp.378-405.

Altman, J. and Bayer, S. (1988). Development of the rat thalamus: III. Time and site of origin and settling pattern of neurons of the reticular nucleus. *The Journal of Comparative Neurology*, 275(3), pp.406-428.

Angevine, J. B., Jr (1970). Time of neuron origin in the diencephalon of the mouse. An autoradiographic study. J. Comp. Neurol, 139,129 -187.

Asanuma, C. and Stanfield, B. (1990). Induction of somatic sensory inputs to the lateral geniculate nucleus in congenitally blind mice and in phenotypically normal mice. *Neuroscience*, 39(3), pp.533-545.

Bavelier, D. and Neville, H. (2002). Cross-modal plasticity: Where and How?. *Nature Reviews Neuroscience*, 3, pp.443-452.

Beurdeley, M., Spatazza, J., Lee, H., Sugiyama, S., Bernard, C., Di Nardo, A., Hensch, T. and Prochiantz, A. (2012). Otx2 Binding to Perineuronal Nets Persistently Regulates Plasticity in the Mature Visual Cortex. *Journal of Neuroscience*, 32(27), pp.9429-9437.

Bishop, G.H. (1959). The relation between nerve fiber size and sensory modality: phylogenetic implications of the afferent innervation of cortex. *The Journal of Nervous and Mental Disease*, 128(2), pp.89-114.

Blackshaw, S., Scholpp, S., Placzek, M., Ingraham, H., Simerly, R. and Shimogori, T. (2010). Molecular Pathways Controlling Development of Thalamus and Hypothalamus: From Neural Specification to Circuit Formation. *Journal of Neuroscience*, 30(45), pp.14925-14930.

Bourassa, J. and Deschenes, M. (1995). Corticothalamic projections from the primary visual cortex in rats: a single fiber study using biocytin as an anterograde tracer. *Neuroscience,* 66, pp. 253-63.

Bourassa, J., Pinault, D. and Deschenes, M. (1995). Corticothalamic projections from the cortical barrel field to the somatosensory thalamus in rats: a single-fibre study using biocytin as an anterograde tracer. *Eur J Neurosci,* 7, pp. 19-30.

Bronchti, G., Heil, P., Sadka, R., Hess, A., Scheich, H. and Wollberg, Z. (2002). Auditory activation of ‘visual’ cortical areas in the blind mole rat (Spalax ehrenbergi). *European Journal of Neuroscience*, 16(2), pp.311-329.

Bronchti, G., Heil, P., Scheich, H. and Wollberg, Z. (1989). Auditory pathway and auditory activation of primary visual targets in the blind mole rat (Spalax ehrenbergi): I. 2-deoxyglucose study of subcortical centers. *The Journal of Comparative Neurology*, 284(2), pp.253-274.

Brooks, J., Su, J., Levy, C., Wang, J., Seabrook, T., Guido, W. and Fox, M. (2013). A Molecular Mechanism Regulating the Timing of Corticogeniculate Innervation. *Cell Reports*, 5(3), pp.573-581.

Butler, A. (2008). Evolution of the thalamus: a morphological and functional review. *Thalamus & Related Systems*, 4(01).

Cang, J., Kaneko, M., Yamada, J., Woods, G., Stryker, M. and Feldheim, D. (2005). Ephrin-As Guide the Formation of Functional Maps in the Visual Cortex. *Neuron*, 48(4), pp.577-589.

Chabot, N., Robert, S., Tremblay, R., Miceli, D., Boire, D. and Bronchti, G. (2007). Audition differently activates the visual system in neonatally enucleated mice compared with anophthalmic mutants. *European Journal of Neuroscience*, 26(8), pp.2334-2348.

Charbonneau, V., Laramée, M., Boucher, V., Bronchti, G. and Boire, D. (2012). Cortical and subcortical projections to primary visual cortex in anophthalmic, enucleated and sighted mice. *European Journal of Neuroscience*, 36(7), pp.2949-2963.

Chatterjee, M. and Li, J. (2012). Patterning and Compartment Formation in the Diencephalon. *Frontiers in Neuroscience*, 6.

Chou, S., Babot, Z., Leingartner, A., Studer, M., Nakagawa, Y. and O'Leary, D. (2013). Geniculocortical Input Drives Genetic Distinctions Between Primary and Higher-Order Visual Areas . *Science*, 340(6137), pp.1239-1242.

Clascá, F., Rubio-Garrido, P. and Jabaudon, D. (2012). Unveiling the diversity of thalamocortical neuron subtypes. *European Journal of Neuroscience*, 35(10), pp.1524-1532.

Cohen, L., Celnik, P., Pascual-Leone, A., Corwell, B., Faiz, L., Dambrosia, J., Honda, M., Sadato, N., Gerloff, C., Catala´, M. and Hallett, M. (1997). Functional relevance of cross-modal plasticity in blind humans. *Nature*, 389(6647), pp.180-183.

Deck, M., Lokmane, L., Chauvet, S., Mailhes, C., Keita, M., Niquille, M., Yoshida, M., Yoshida, Y., Lebrand, C., Mann, F., Grove, E. and Garel, S. (2013). Pathfinding of Corticothalamic Axons Relies on a Rendezvous with Thalamic Projections. *Neuron*, 77(3), pp.472-484.

Deschênes, M., Veinante, P. and Zhang, Z. (1998). The organization of corticothalamic projections: reciprocity versus parity. *Brain Research Reviews*, 28(3), pp.286-308.

Deschênes, M., Bourassa, J. and Pinault, D. (1994). Corticothalamic projections from layer V cells in rat are collaterals of long-range corticofugal axons. *Brain Research*, 664(1-2), pp.215-219.

Diao, Y., Cui, L., Chen, Y., Burbridge, T., Han, W., Wirth, B., Sestan, N., Crair, M. and Zhang, J. (2017). Reciprocal Connections Between Cortex and Thalamus Contribute to Retinal Axon Targeting to Dorsal Lateral Geniculate Nucleus. *Cerebral Cortex*, 28(4), pp.1168-1182.

Dufour, A., Seibt, J., Passante, L., Depaepe, V., Ciossek, T., Frisén, J., Kullander, K., Flanagan, J., Polleux, F. and Vanderhaeghen, P. (2003). Area Specificity and Topography of Thalamocortical Projections Are Controlled by ephrin/Eph Genes. *Neuron*, 39(3), pp.453-465.

Ellsworth, C., Lyckman, A., Feldheim, D., Flanagan, J. and Sur, M. (2005). Ephrin-A2 and -A5 influence patterning of normal and novel retinal projections to the thalamus: Conserved mapping mechanisms in visual and auditory thalamic targets. *The Journal of Comparative Neurology*, 488(2), pp.140-151.

Frangeul, L., Pouchelon, G., Telley, L., Lefort, S., Luscher, C. and Jabaudon, D. (2016). A cross-modal genetic framework for the development and plasticity of sensory pathways. *Nature*, 538(7623), pp.96-98.

Gao, P., Postiglione, M., Krieger, T., Hernandez, L., Wang, C., Han, Z., Streicher, C., Papusheva, E., Insolera, R., Chugh, K., Kodish, O., Huang, K., Simons, B., Luo, L., Hippenmeyer, S. and Shi, S. (2014). Deterministic Progenitor Behavior and Unitary Production of Neurons in the Neocortex. *Cell*, 159(4), pp.775-788.

Gezelius, H., Moreno-Juan, V., Mezzera, C., Thakurela, S., Rodríguez-Malmierca, L., Pistolic, J., Benes, V., Tiwari, V. and López-Bendito, G. (2016). Genetic Labeling of Nuclei-Specific Thalamocortical Neurons Reveals Putative Sensory-Modality Specific Genes. *Cerebral Cortex.*

Godement, P., Salaün, J. and Imbert, M. (1984). Prenatal and postnatal development of retinogeniculate and retinocollicular projections in the mouse. *Journal of Comparative Neurology*, 230(4), pp.552-575.

Golding, B., Pouchelon, G., Bellone, C., Murthy, S., Di Nardo, A., Govindan, S., Ogawa, M., Shimogori, T., Lüscher, C., Dayer, A. and Jabaudon, D. (2014). Retinal Input Directs the Recruitment of Inhibitory Interneurons into Thalamic Visual Circuits. *Neuron*, 81(6), p.1443.

Goldstein, S., Bockenhauer, D., O'Kelly, I. and Zilberberg, N. (2001). Potassium leak channels and the KCNK family of two-p-domain subunits. *Nature Reviews Neuroscience*, 2(3), pp.175-184.

Grant, E., Hoerder-Suabedissen, A. and Molnár, Z. (2016). The Regulation of Corticofugal Fiber Targeting by Retinal Inputs. *Cerebral Cortex*, 26(3), pp.1336-1348.

Guillery, R. and Sherman, S. (2002). Thalamic Relay Functions and Their Role in Corticocortical Communication. *Neuron*, 33(2), pp.163-175.

Homman-Ludiye, J. and Bourne, J. (2014). Mapping arealisation of the visual cortex of non-primate species: lessons for development and evolution. *Frontiers in Neural Circuits*, 8.

Horng, S., Kreiman, G., Ellsworth, C., Page, D., Blank, M., Millen, K. and Sur, M. (2009). Differential Gene Expression in the Developing Lateral Geniculate Nucleus and Medial Geniculate Nucleus Reveals Novel Roles for Zic4 and Foxp2 in Visual and Auditory Pathway Development. *Journal of Neuroscience*, 29(43), pp.13672-13683.

Horng, S. and Sur, M. (2006). Visual activity and cortical rewiring: activity-dependent plasticity of cortical networks. *Progress in Brain Research*, pp.3-381.

Huberman, A., Feller, M. and Chapman, B. (2008). Mechanisms Underlying Development of Visual Maps and Receptive Fields. *Annual Review of Neuroscience*, 31(1), pp.479-509.

Hunnicutt, B., Long, B., Kusefoglu, D., Gertz, K., Zhong, H. and Mao, T. (2014). A comprehensive thalamocortical projection map at the mesoscopic level. *Nature Neuroscience*, 17(9), pp.1276-1285.

Inamura, N., Ono, K., Takebayashi, H., Zalc, B. and Ikenaka, K. (2011). Olig2 Lineage Cells Generate GABAergic Neurons in the Prethalamic Nuclei, Including the Zona Incerta, Ventral Lateral Geniculate Nucleus and Reticular Thalamic Nucleus. *Developmental Neuroscience*, 33(2), pp.118-129.

Izraeli, R., Koay, G., Lamish, M., Heicklen-Klein, A., Heffner, H., Heffner, R. and Wollberg, Z. (2002). Cross-modal neuroplasticity in neonatally enucleated hamsters: structure, electrophysiology and behaviour. *European Journal of Neuroscience*, 15(4), pp.693-712.

Jeong, Y., Dolson, D., Waclaw, R., Matise, M., Sussel, L., Campbell, K., Kaestner, K. and Epstein, D. (2011). Spatial and temporal requirements for sonic hedgehog in the regulation of thalamic interneuron identity. *Development*, 138(3), pp.531-541.

Jones, E. (2007). The thalamus. *Cambridge: Cambridge University Press*.

Kiecker, C. and Lumsden, A. (2004). Hedgehog signaling from the ZLI regulates diencephalic regional identity. Nature Neuroscience, 7(11), pp.1242-1249.

Laramée, M., Bronchti, G. and Boire, D. (2013). Primary visual cortex projections to extrastriate cortices in enucleated and anophthalmic mice. *Brain Structure and Function*, 219(6), pp.2051-2070.

Lim, Y. and Golden, J. (2007). Patterning the developing diencephalon. *Brain Research Reviews*, 53(1), pp.17-26.

López-Bendito, G. and Molnár, Z. (2003). Erratum: Thalamocortical development: how are we going to get there?. *Nature Reviews Neuroscience*, 4(5), pp.422-422.

Martinez-Ferre, A. and Martinez, S. (2012). Molecular Regionalization of the Diencephalon. *Frontiers in Neuroscience*, 6.

Molnár, Z., Garel, S., López-Bendito, G., Maness, P. and Price, D. (2012). Mechanisms controlling the guidance of thalamocortical axons through the embryonic forebrain. *European Journal of Neuroscience*, 35(10), pp.1573-1585.

Mooney RD and Rhoades RW (1983) Neonatal enucleation alters functional organization in hamster's lateral posterior nucleus. *Brain Res* (285):399-404.

Moreno-Juan, V., Filipchuk, A., Antón-Bolaños, N., Mezzera, C., Gezelius, H., Andrés, B., Rodríguez-Malmierca, L., Susín, R., Schaad, O., Iwasato, T., Schüle, R., Rutlin, M., Nelson, S., Ducret, S., Valdeolmillos, M., Rijli, F. and López-Bendito, G. (2017). Prenatal thalamic waves regulate cortical area size prior to sensory processing. *Nature Communications*, 8, p.14172.

Nagalski, A., Puelles, L., Dabrowski, M., Wegierski, T., Kuznicki, J. and Wisniewska, M. (2015). Molecular anatomy of the thalamic complex and the underlying transcription factors. *Brain Structure and Function*, 221(5), pp.2493-2510.

Nakagawa, Y. and Shimogori, T. (2012). Diversity of thalamic progenitor cells and postmitotic neurons. *European Journal of Neuroscience*, 35(10), pp.1554-1562.

Nakagawa, Y. and O'Leary, D. D. (2001). Combinatorial expression patterns of LIM-homeodomain and other regulatory genes parcellate developing thalamus. *J. Neurosci*, 21,2711 -2725.

Négyessy, L., Gál, V., Farkas, T. and Toldi, J. (2000). Cross-modal plasticity of the corticothalamic circuits in rats enucleated on the first postnatal day. *European Journal of Neuroscience*, 12(5), pp.1654-1668.

Piché, M., Chabot, N., Bronchti, G., Miceli, D., Lepore, F. and Guillemot, J. (2007). Auditory responses in the visual cortex of neonatally enucleated rats. *Neuroscience*, 145(3), pp.1144-1156.

Piscopo, D., El-Danaf, R., Huberman, A. and Niell, C. (2013). Diverse Visual Features Encoded in Mouse Lateral Geniculate Nucleus. *Journal of Neuroscience*, 33(11), pp.4642-4656.

Pouchelon, G., Gambino, F., Bellone, C., Telley, L., Vitali, I., Lüscher, C., Holtmaat, A. and Jabaudon, D. (2014). Modality-specific thalamocortical inputs instruct the identity of postsynaptic L4 neurons. *Nature*, 511(7510), pp.471-474.

Puelles, L. and Rubenstein, J. (2003). Forebrain gene expression domains and the evolving prosomeric model. *Trends in Neurosciences*, 26(9), pp.469-476.

Rauschecker, J. (1995). Compensatory plasticity and sensory substitution in the cerebral cortex. *Trends in Neurosciences*, 18(1), pp.36-43.

Roe, A., Pallas, S., Kwon, Y. and Sur, M. (1992). Visual projections routed to the auditory pathway in ferrets: receptive fields of visual neurons in primary auditory cortex. *The Journal of Neuroscience*, 12(9), pp.3651-3664.

Rouiller, E. and Welker, E. (1991). Morphology of corticothalamic terminals arising from the auditory cortex of the rat: A Phaseolus vulgaris-leucoagglutinin (PHA-L) tracing study. *Hearing Research*, 56(1-2), pp.179-190.

Saalmann, Y. and Kastner, S. (2011). Cognitive and Perceptual Functions of the Visual Thalamus*. Neuron*, 71(2), pp.209-223.

Scholpp, S. and Lumsden, A. (2010). Building a bridal chamber: development of the thalamus. *Trends in Neurosciences*, 33(8), pp.373-380.

Seabrook, T., El-Danaf, R., Krahe, T., Fox, M. and Guido, W. (2013). Retinal Input Regulates the Timing of Corticogeniculate Innervation. *Journal of Neuroscience*, 33(24), pp.10085-10097.

Shanks, J., Ito, S., Schaevitz, L., Yamada, J., Chen, B., Litke, A. and Feldheim, D. (2016). Corticothalamic Axons Are Essential for Retinal Ganglion Cell Axon Targeting to the Mouse Dorsal Lateral Geniculate Nucleus. *The Journal of Neuroscience*, 36(19), pp.5252-5263.

Sherman, S. and Guillery, R. (2011). Distinct functions for direct and transthalamic corticocortical connections. *Journal of Neurophysiology*, 106(3), pp.1068-1077.

Sherman, S. and Guillery, R. (2006). Exploring the thalamus and its role in cortical function. *Cambridge, Mass.: MIT Press*.

Sherman, S. and Guillery, R. (2002). The role of the thalamus in the flow of information to the cortex. *Philosophical Transactions of the Royal Society B: Biological Sciences*, 357(1428), pp.1695-1708.

Shi, W., Xianyu, A., Han, Z., Tang, X., Li, Z., Zhong, H., Mao, T., Huang, K. and Shi, S. (2017). Ontogenetic establishment of order-specific nuclear organization in the mammalian thalamus. *Nature Neuroscience*, 20(4), pp.516-528.

Singh, R., Su, J., Brooks, J., Terauchi, A., Umemori, H. and Fox, M. (2012). Fibroblast Growth Factor 22 Contributes to the Development of Retinal Nerve Terminals in the Dorsal Lateral Geniculate Nucleus. *Frontiers in Molecular Neuroscience*, 4.

Staudt, N. and Houart, C. (2007). The Prethalamus Is Established during Gastrulation and Influences Diencephalic Regionalization. *PLoS Biology*, 5(4), p.e69.

Sugiyama, S., Di Nardo, A., Aizawa, S., Matsuo, I., Volovitch, M., Prochiantz, A. and Hensch, T. (2008). Experience-Dependent Transfer of Otx2 Homeoprotein into the Visual Cortex Activates Postnatal Plasticity. *Cell*, 134(3), pp.508-520.

Suzuki-Hirano, A., Ogawa, M., Kataoka, A., Yoshida, A., Itoh, D., Ueno, M., Blackshaw, S. and Shimogori, T. (2010). Dynamic spatiotemporal gene expression in embryonic mouse thalamus. *The Journal of Comparative Neurology*, 519(3), pp.528-543.

Thompson, A., Picard, N., Min, L., Fagiolini, M. and Chen, C. (2016). Cortical Feedback Regulates Feedforward Retinogeniculate Refinement. *Neuron*, 91(5), pp.1021-1033.

Toldi, J., Feher, O. and Wolff, J. (1996). Neuronal plasticity induced by neonatal monocular (and binocular) enucleation. *Progress in Neurobiology*, 48(3), pp.191-218.

Toldi, J., Rojik, I. and Fehér, O. (1994). Neonatal monocular enucleation-induced cross-modal effects observed in the cortex of adult rat. *Neuroscience*, 62(1), pp.105-114.

Vanderhaeghen, P., Lu, Q., Prakash, N., Frisén, J., Walsh, C., Frostig, R. and Flanagan, J. (2000). A mapping label required for normal scale of body representation in the cortex. *Nature Neuroscience*, 3(4), pp.358-365.

Vue, T., Aaker, J., Taniguchi, A., Kazemzadeh, C., Skidmore, J., Martin, D., Martin, J., Treier, M. and Nakagawa, Y. (2007). Characterization of progenitor domains in the developing mouse thalamus. *The Journal of Comparative Neurology*, 505(1), pp.73-91.

Wilks, T., Harvey, A. and Rodger, J. (2013). Seeing with Two Eyes: Integration of Binocular Retinal Projections in the Brain. *Functional Brain Mapping and the Endeavor to Understand the Working Brain*.

Wong, S., Scott, E., Mu, W., Guo, X., Borgenheimer, E., Freeman, M., Ming, G., Wu, Q., Song, H. and Nakagawa, Y. (2018). In vivo clonal analysis reveals spatiotemporal regulation of thalamic nucleogenesis. *PLOS Biology*, 16(4), p.e2005211.

Yaka, R., Yinon, U. and Wollberg, Z. (1999). Auditory activation of cortical visual areas in cats after early visual deprivation. *European Journal of Neuroscience*, 11(4), pp.1301-1312.